

Level Structure of $^{32,34}\text{P}$: What do we learn about the $f_{7/2} - p_{3/2}$ energy gap ?

Sandeep. S. Ghugre

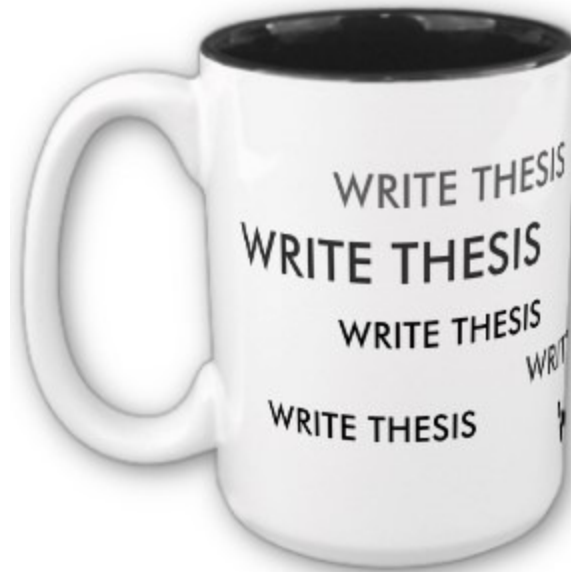
UGC-DAE Consortium for Scientific Research
Kolkata Centre



© Original Artist
Reproduction rights obtainable from
www.CartoonStock.com,



search ID: rb0n69



RITWIKA CHAKRABARTI



**Dr. A. K. Sinha, Prof. Umesh Garg, Prof . Alex Brown,
Co-authors.....**

Mr. K. Basu, INGA Collaboration

Dr. W. P. Tan, Dr. Larry Lamm, Mr. J. P. Greene

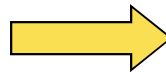
Introduction & Motivation



inversion



Shell structure:
Nucleon motion in mean field



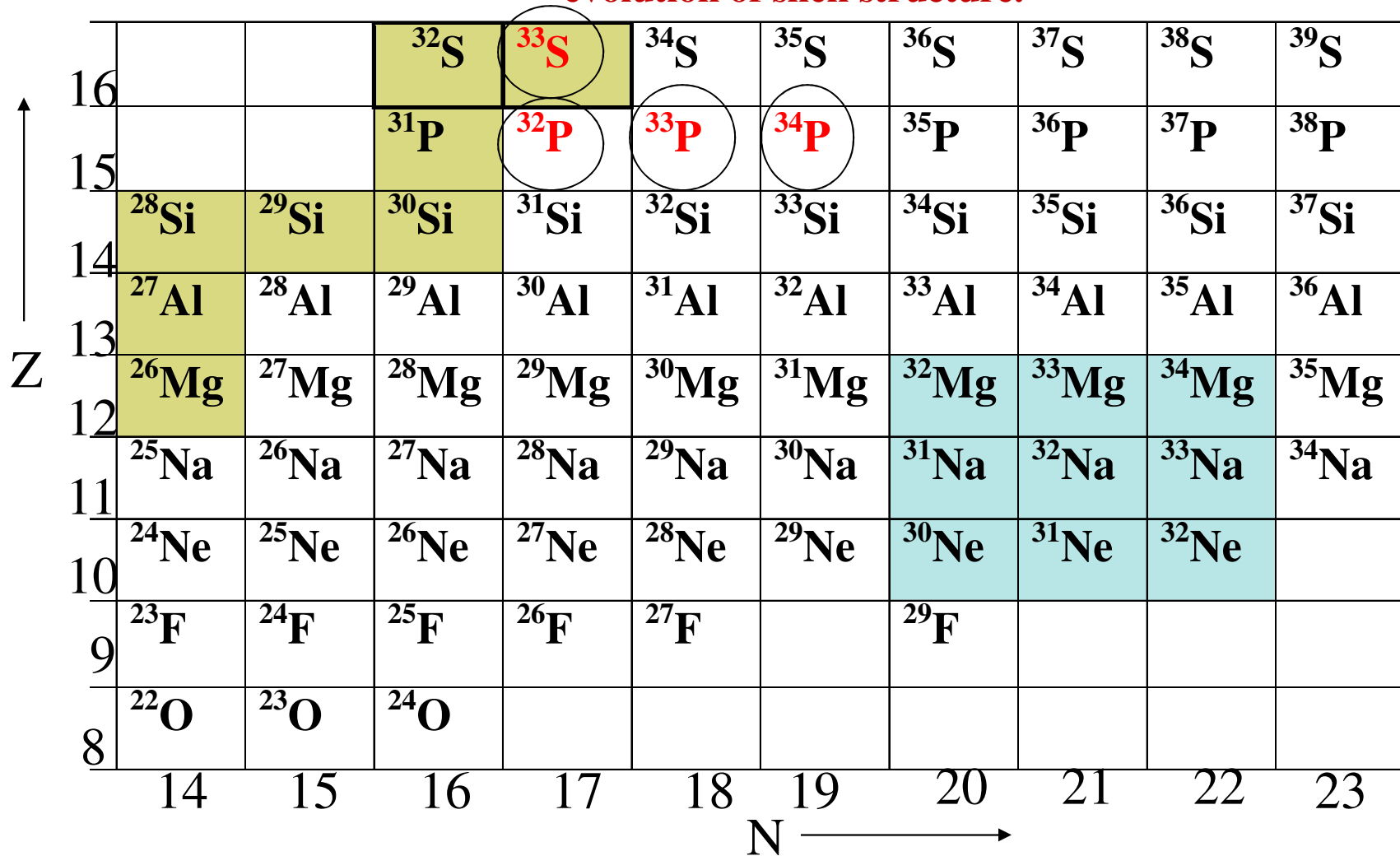
Inversion:
Domination of residual nucleon-nucleon
interaction

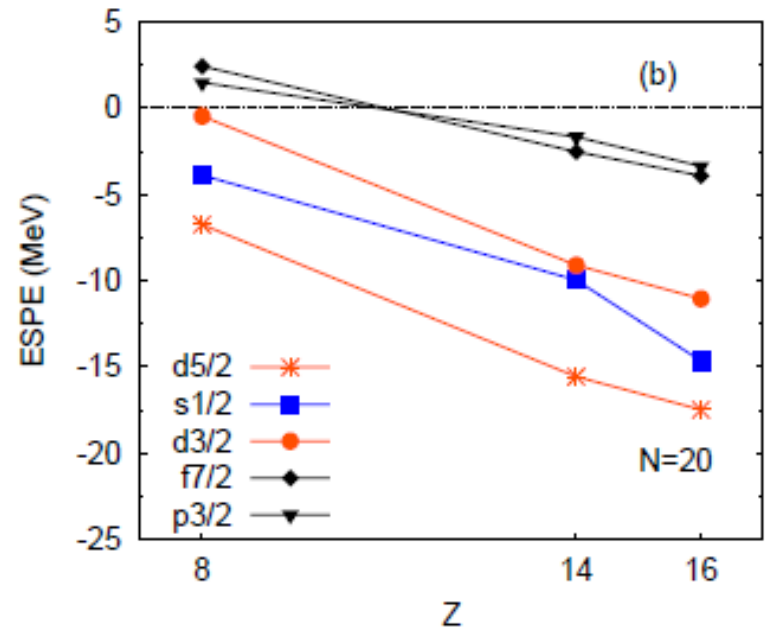
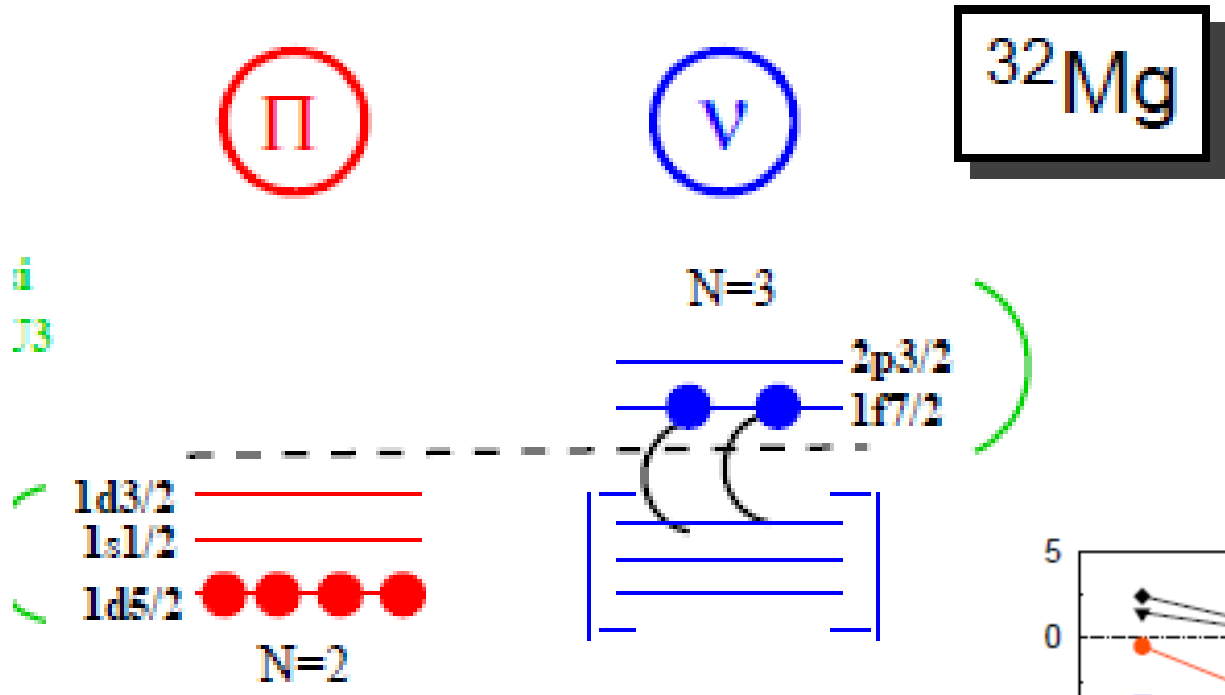
What happens to the nuclear structure in between the valley of stability
And the island of inversion?

The region between: **The valley of stability** & **Island of Inversion**

is a highly transitional region

Investigations into the extent of the island of inversion and the transition from stable nuclei to neutron-rich nuclei will lead to a greater understanding of the evolution of shell structure.





In fact, the shell does evolve, due to the **tensor force**.

[Otsuka et al., *PRL* 95 (05) 232502]

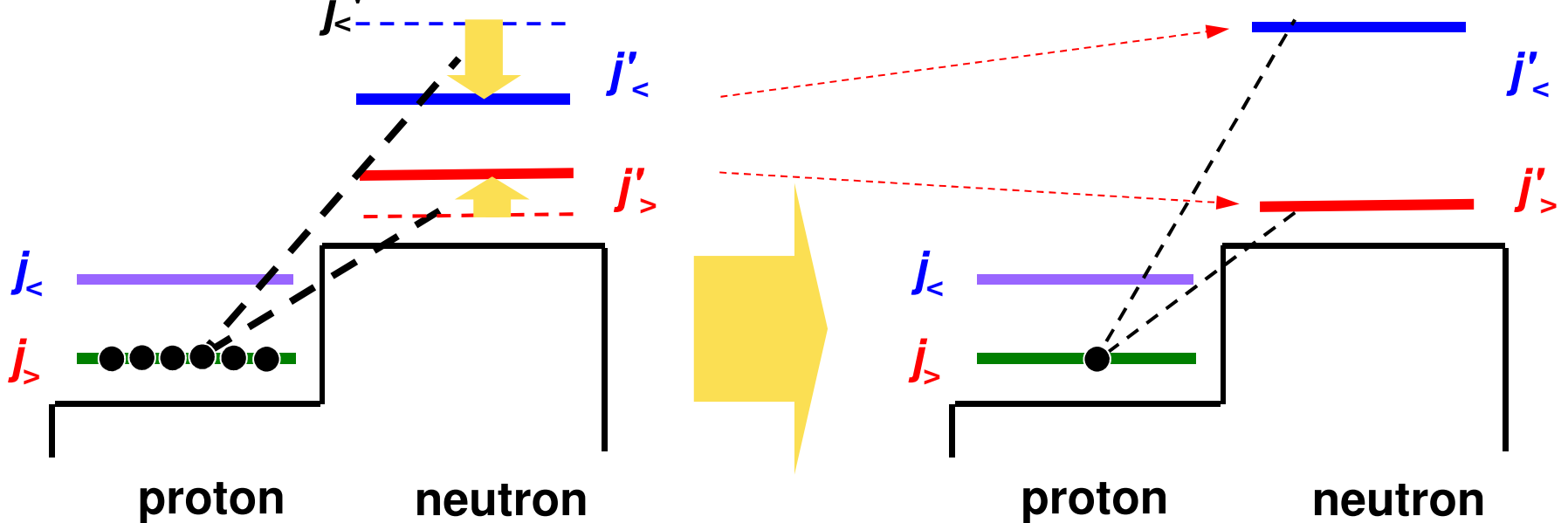
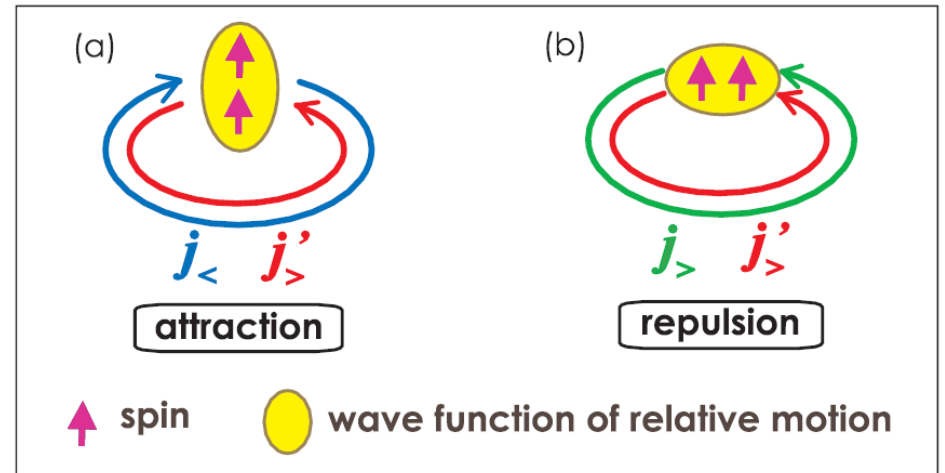
[Otsuka et al., *PRL* 97 (06) 162501]

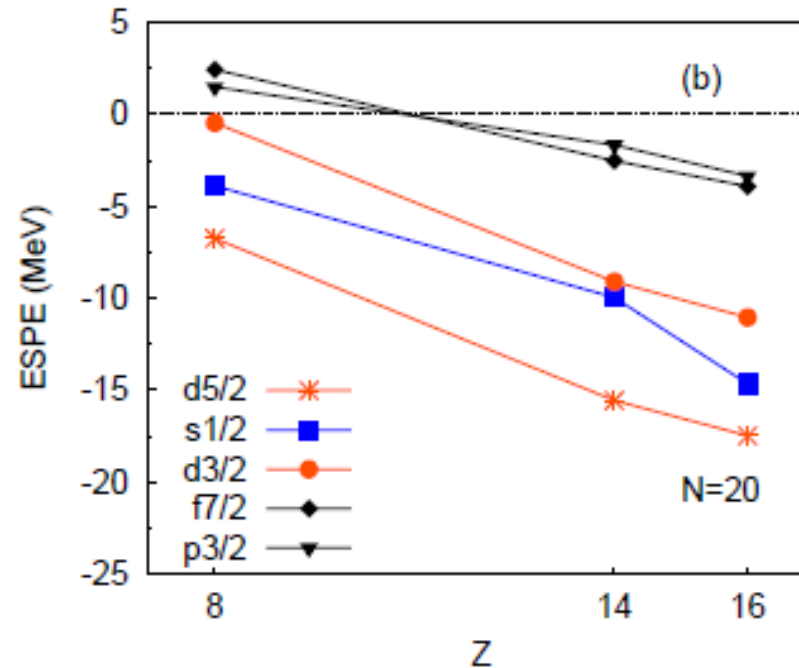
- Monopole energy of the tensor interaction

$$V_{j,j'}^T = \frac{\sum_J (2J+1) \langle jj' | V | jj' \rangle_{JT}}{\sum_J (2J+1)}$$

is

- attractive for $j_> - j_<', j_< - j_>'$
- repulsive for $j_> - j_>', j_< - j_<'$





Thus, the single-particle orbits may migrate leading to a possible change in shell structure.

Important to have experimental spectroscopic study in this transitional region of the nuclear landscape

Level Energy

Spin

Parity

Lifetimes



γ^n matrices

Angular Correlation

Polarization

Lineshape

Test of shell models

Whether the N=20 shell gap decreases here?

Is there a need to decrease SPE'S for these nuclei?

How to populate neutron-rich nuclei?

Reactions employed in earlier investigations of nuclei in the vicinity of the island of inversion

β -decay

Nathan et al, PRC 15,1448(1977)

Deuteron inelastic scattering

I.Iwasa et al., PRC67 (2003)064315

Heavy ion collision

Fornal et al PRC49 ,2413(1994)

Deep inelastic

R.Broda, J.Phys.G32,R151(2006)

Intermediate energy coulomb excitation

Pritychenko et al, PRC62,051601®(2000)

Transfer/deep inelastic

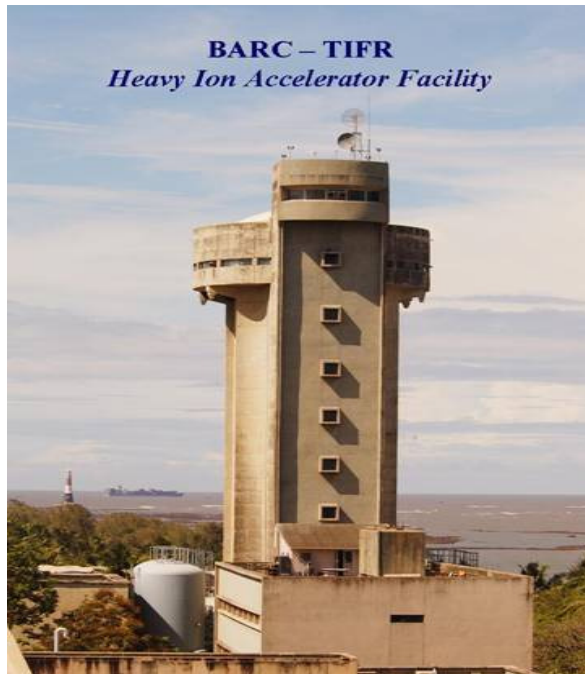
Krishichayan et al, Eur.Phys.J.A29,151(2006)

**Limited in terms of population of higher angular momentum states.
Coincident binary emission has to be taken care of for transfer/deep inelastic reaction.
Complicated setup and more presorting required**

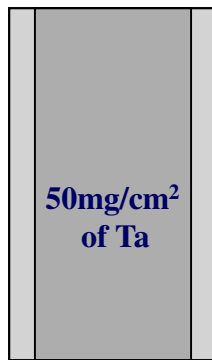
Solution:

Use **Fusion-evaporation reaction** using a neutron-rich target and/or a neutron-rich projectile

Experimental Details



$^{18}\text{O} + ^{18}\text{O} @ 34\text{MeV}$



TARGET

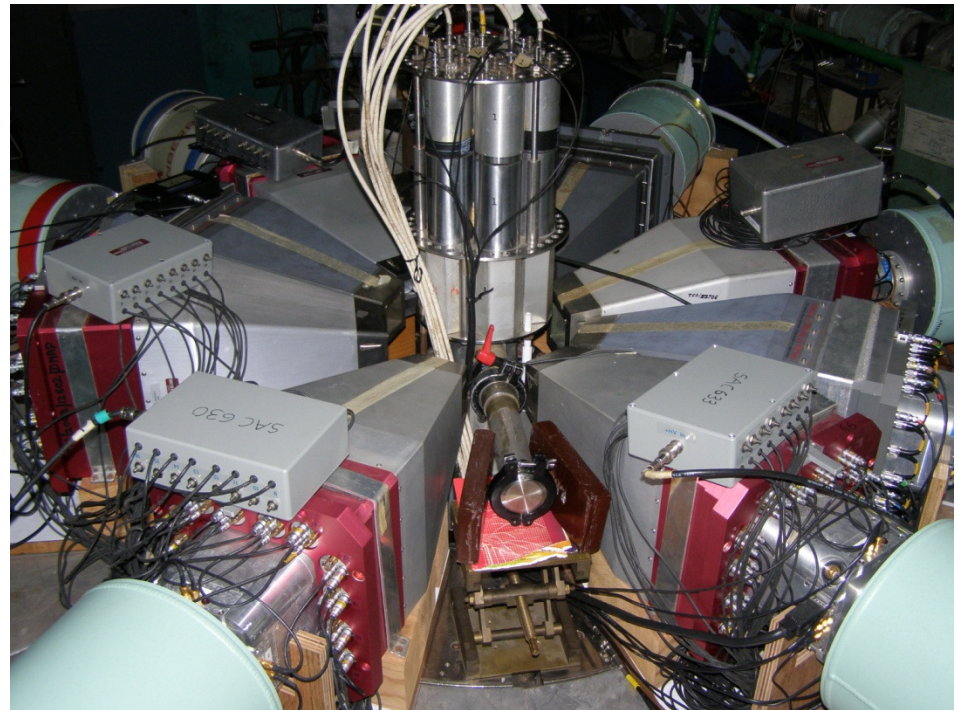
^{18}O (thickness
~1.6mg/cm²)

An event was recorded when :
Two clovers fire in coincidence

Detector Array

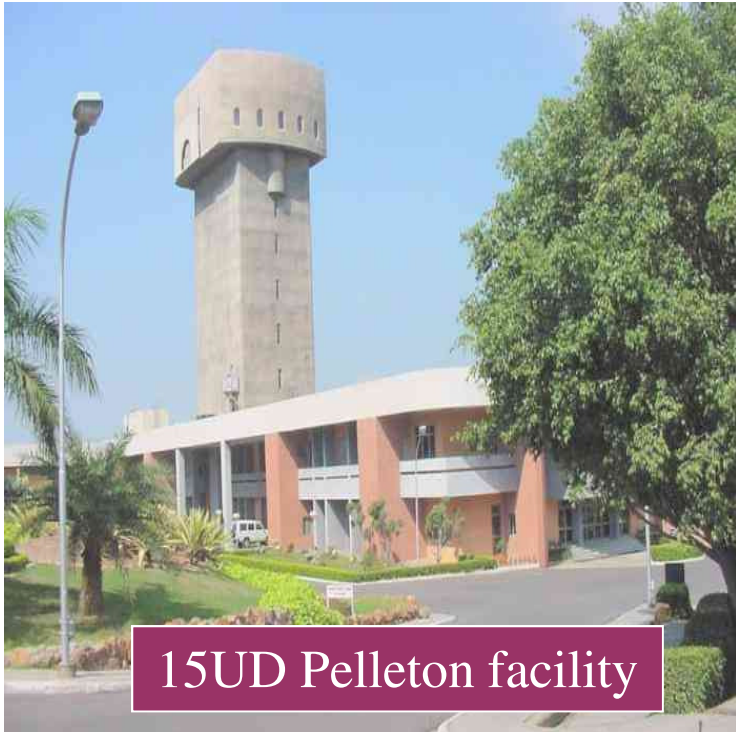
Beam	^{18}O
Beam current	~ 20 nA
Beam energy	34 MeV
Target	^{18}O (Tantalum Oxide)
Detector configuration	7CLOVER detectors
Event rate	~ 1.3k/s
Events recorded	~1 Billion γ - γ coincidences

DATA Acquisition System:
CAMAC Based multi-parameter system "**LAMPS**"



$^{16}\text{O}+^{18}\text{O}@34\text{MeV}$

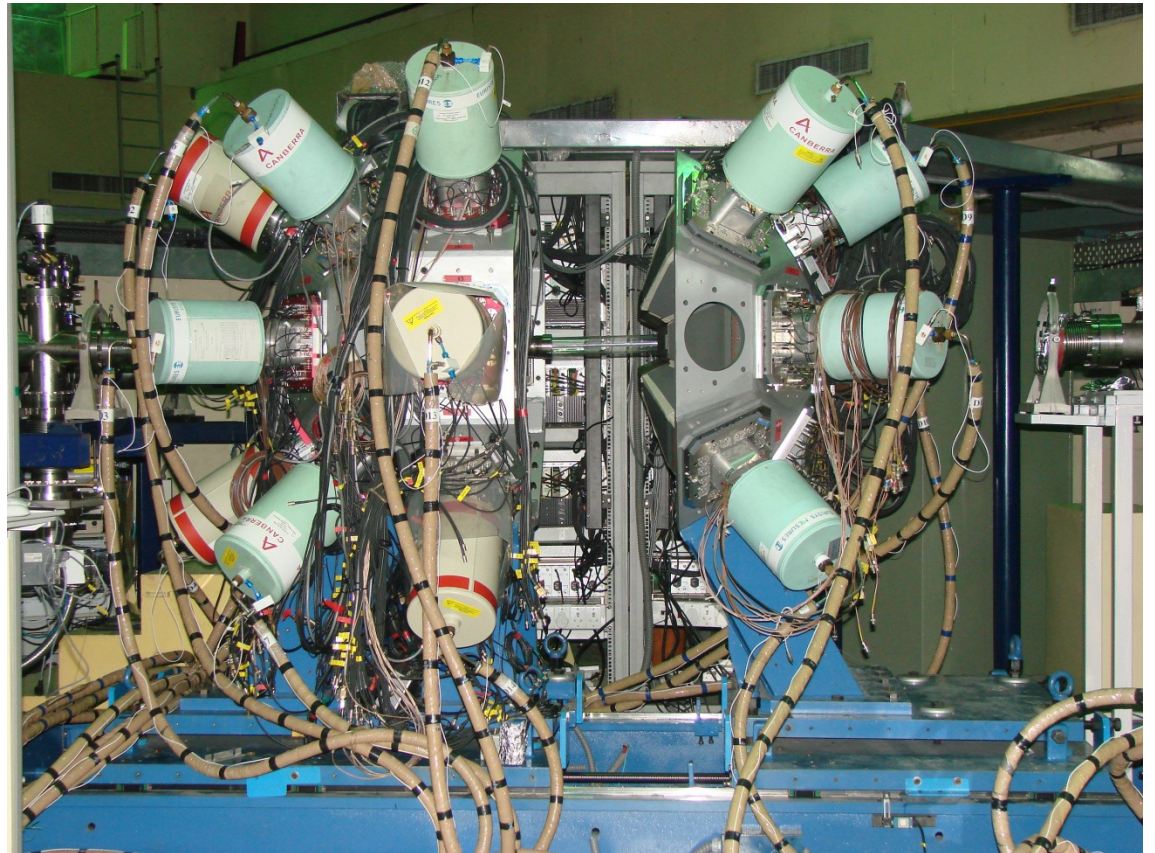
INDIAN NATIONAL GAMMA ARRAY



15UD Pelleton facility

Inter University Accelerator
Centre, New Delhi

18 Clover detectors:
3 at $\sim 32^\circ$, 4 at $\sim 57^\circ$,
5 at $\sim 90^\circ$, 3 at $\sim 123^\circ$,
3 at $\sim 148^\circ$.



Fusion-evaporation has resulted in considerable enhancement of production of ^{34}P

Krishichayan *et al* EPJA 29,151 (2006)

Transfer Reactions/Deep-inelastic Reactions

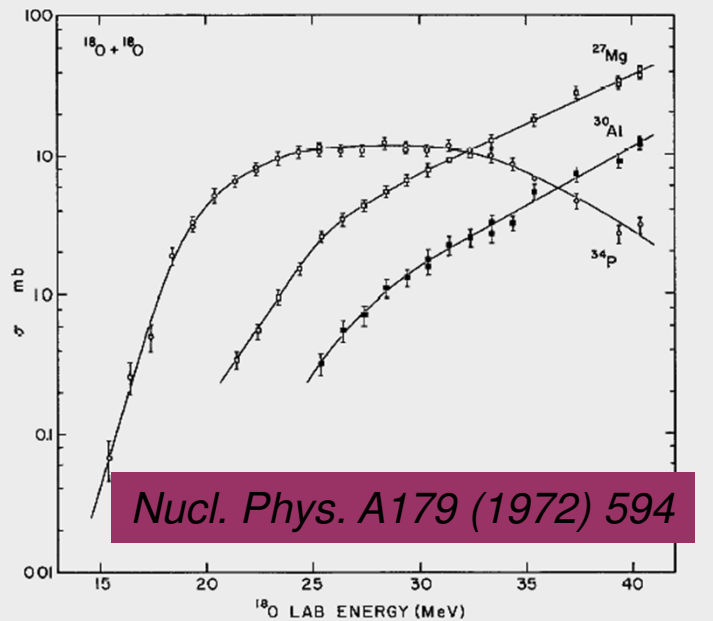
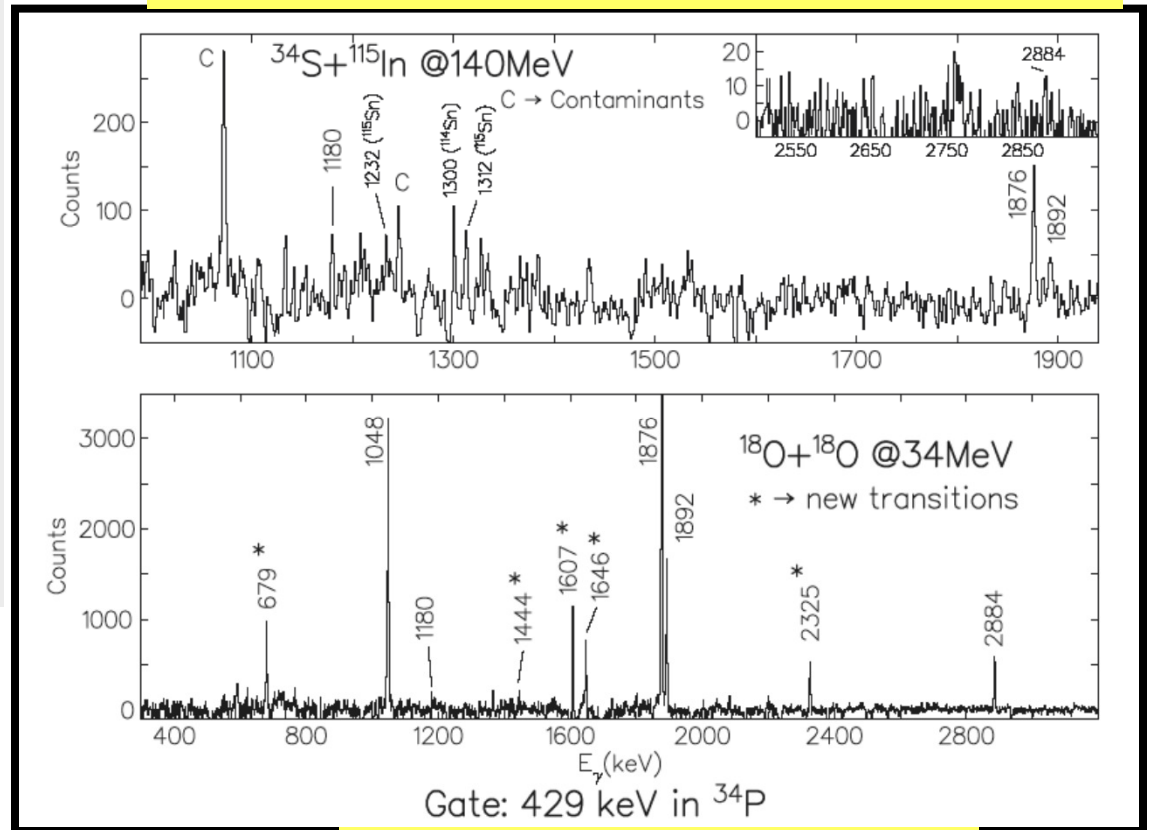


Fig. 3. Excitation function of the residual nuclei ^{27}Mg , ^{30}Al and ^{34}P produced in the compound-nucleus reaction $^{18}\text{O} + ^{18}\text{O}$.

Excitation function of residual nuclei produced in the compound nuclear Reaction $^{18}\text{O} + ^{18}\text{O}$.

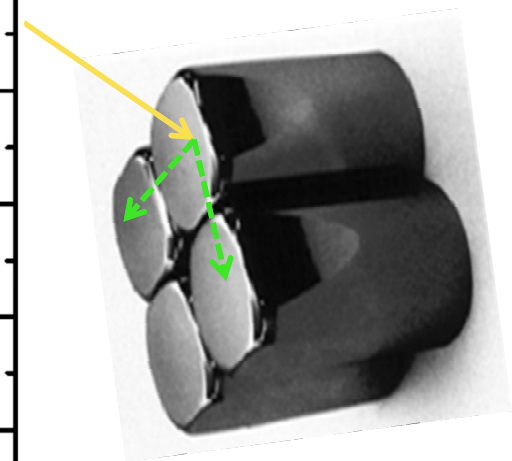
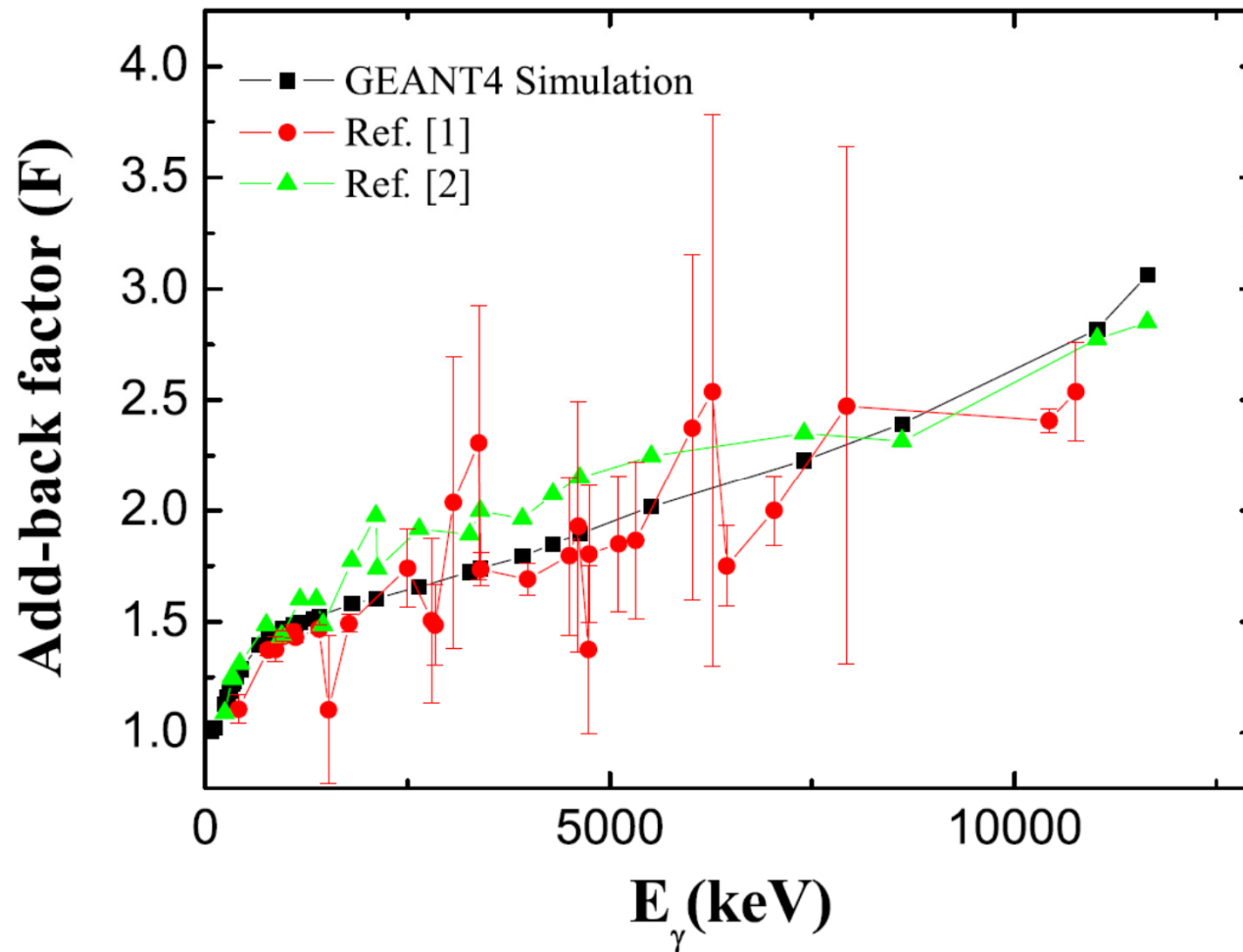


Fusion-evaporation channel

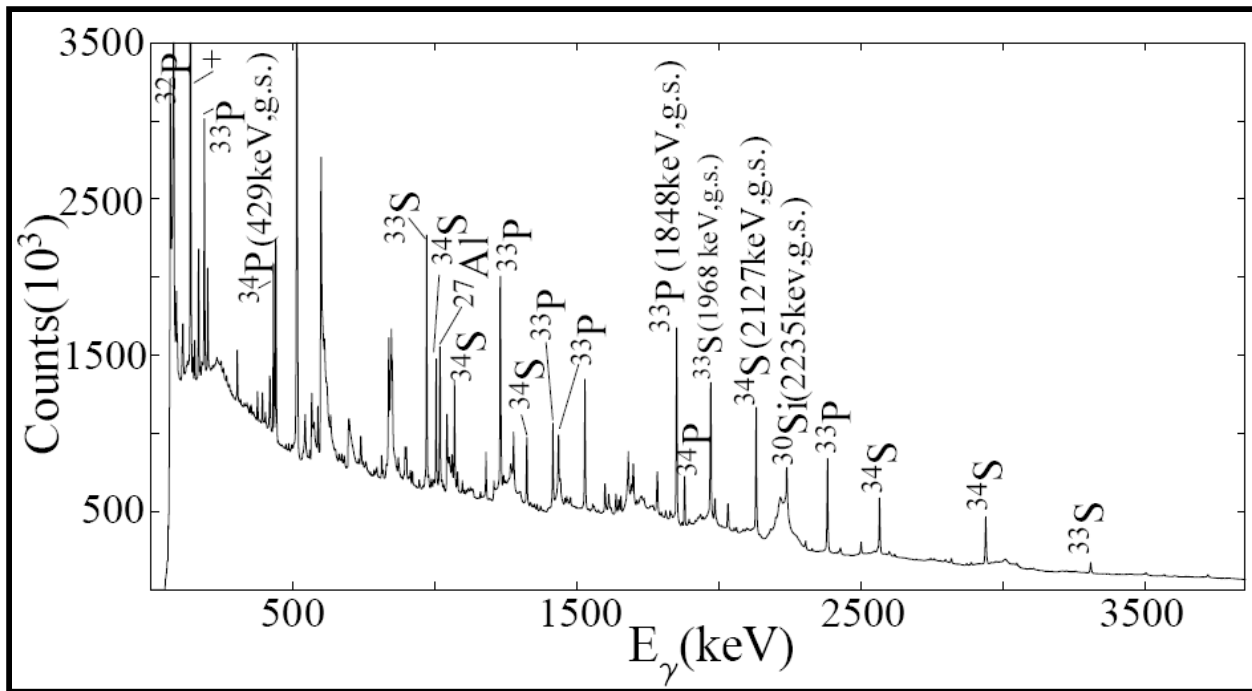
R. Chakrabarti *et al* PRC 80, 034326 (2009)

How to investigate the structure of the Nucleus?

In-beam Gamma ray spectroscopy



Results

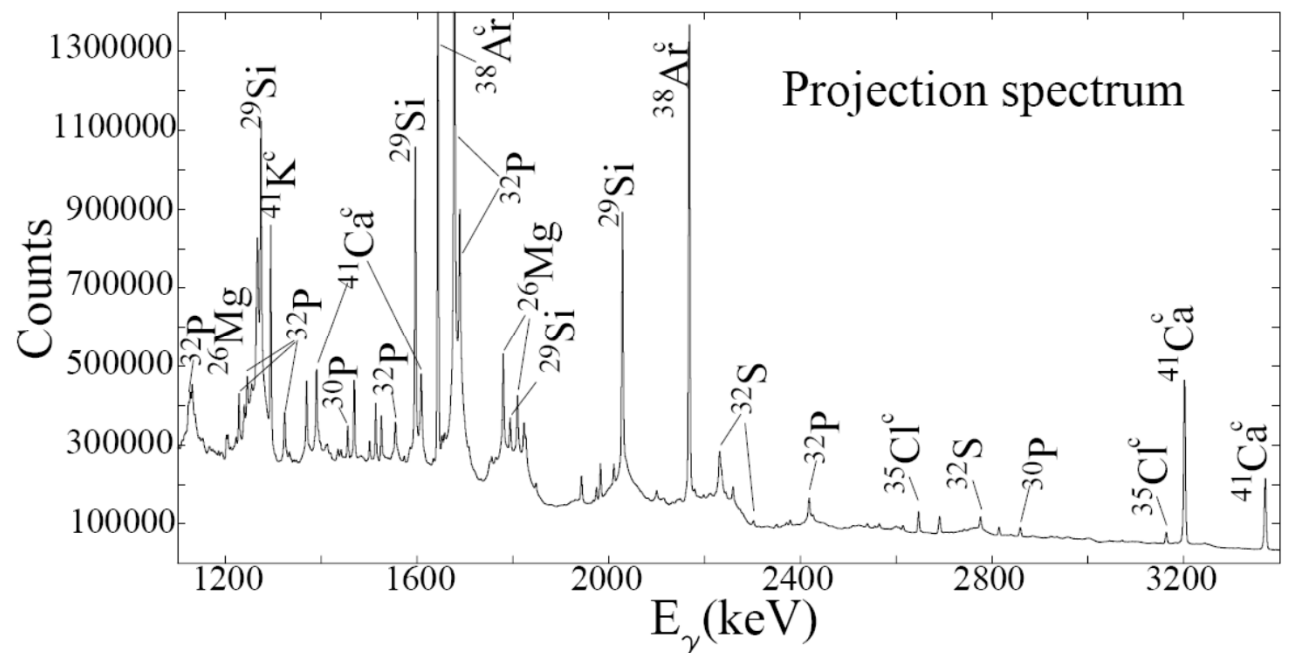


Projection spectrum:
 $^{18}\text{O} + ^{18}\text{O}$ @ 34 MeV

Populated nuclei:
 $^{33,34}\text{S}$, $^{33,34}\text{P}$, $^{30,31,32}\text{Si}$

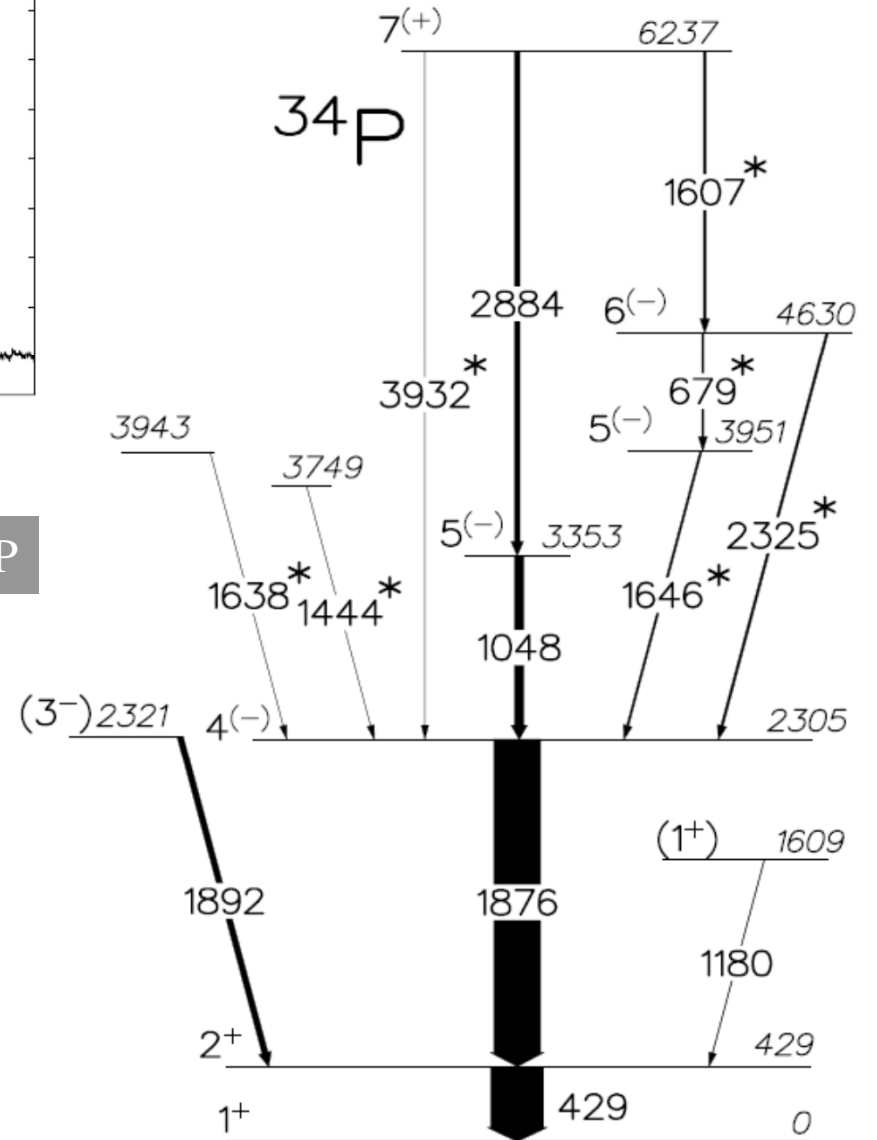
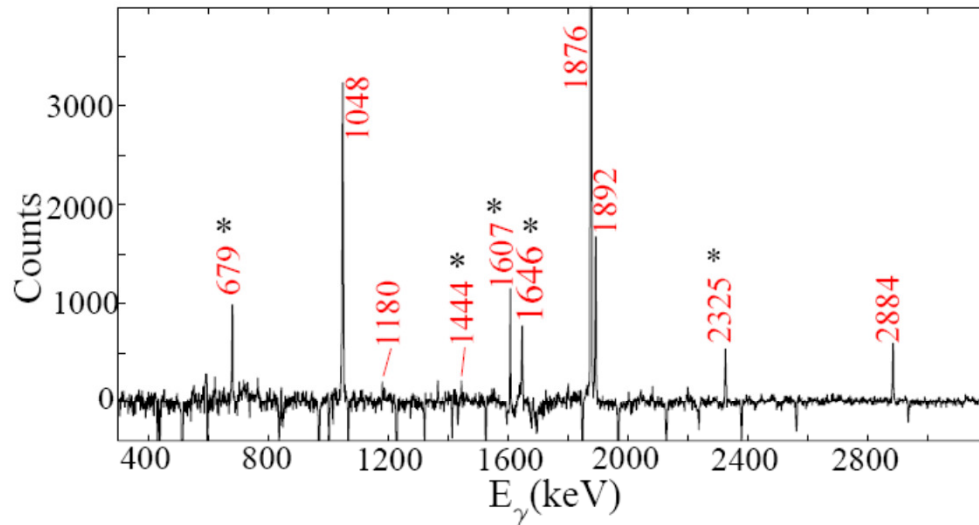
Projection spectrum:
 $^{16}\text{O} + ^{18}\text{O}$ @ 34 MeV

Populated nuclei:
 ^{32}S , $^{30,31,32}\text{P}$, $^{29,30}\text{Si}$



Projection spectrum

From $^{18}\text{O} + ^{18}\text{O}$ @ 34 MeV



Phys. Rev. C 80, 034326 (2009)

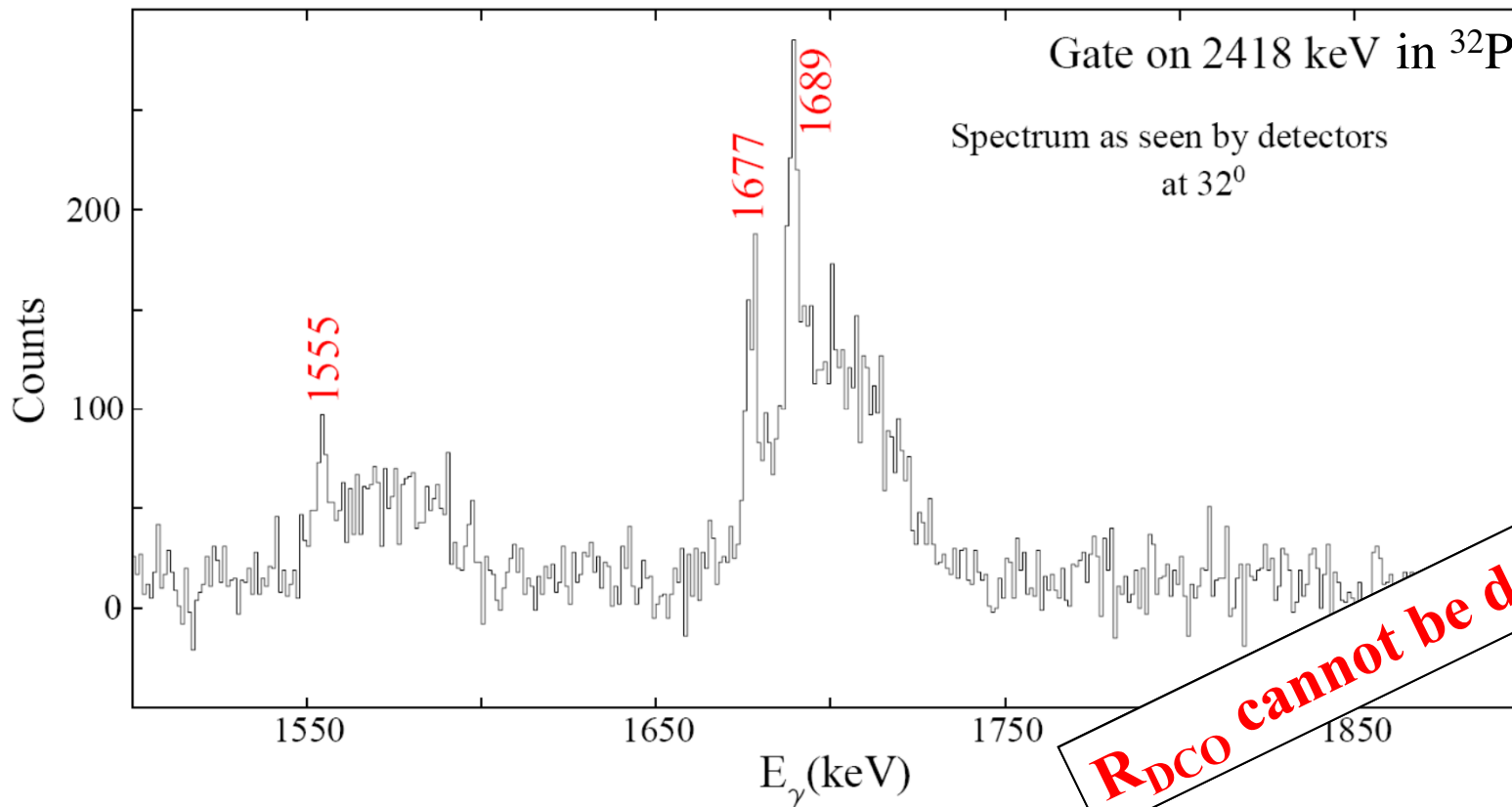
Determination of Multipolarity

$^{16}\text{O} + ^{18}\text{O} @ 34\text{MeV}$

Standard Method:

$$R_{\text{DCO}} = \frac{I_{\gamma_1 \text{ at } 32^\circ \text{ or } 148^\circ, \text{ gated with } \gamma_2 \text{ at } 90^\circ}}{I_{\gamma_1 \text{ at } 90^\circ, \text{ gated with } \gamma_2 \text{ at } 32^\circ \text{ or } 148^\circ}}$$

Gate on 1677 keV or 1689 keV at detectors at 32° or 148°
not possible due to Doppler effects !!



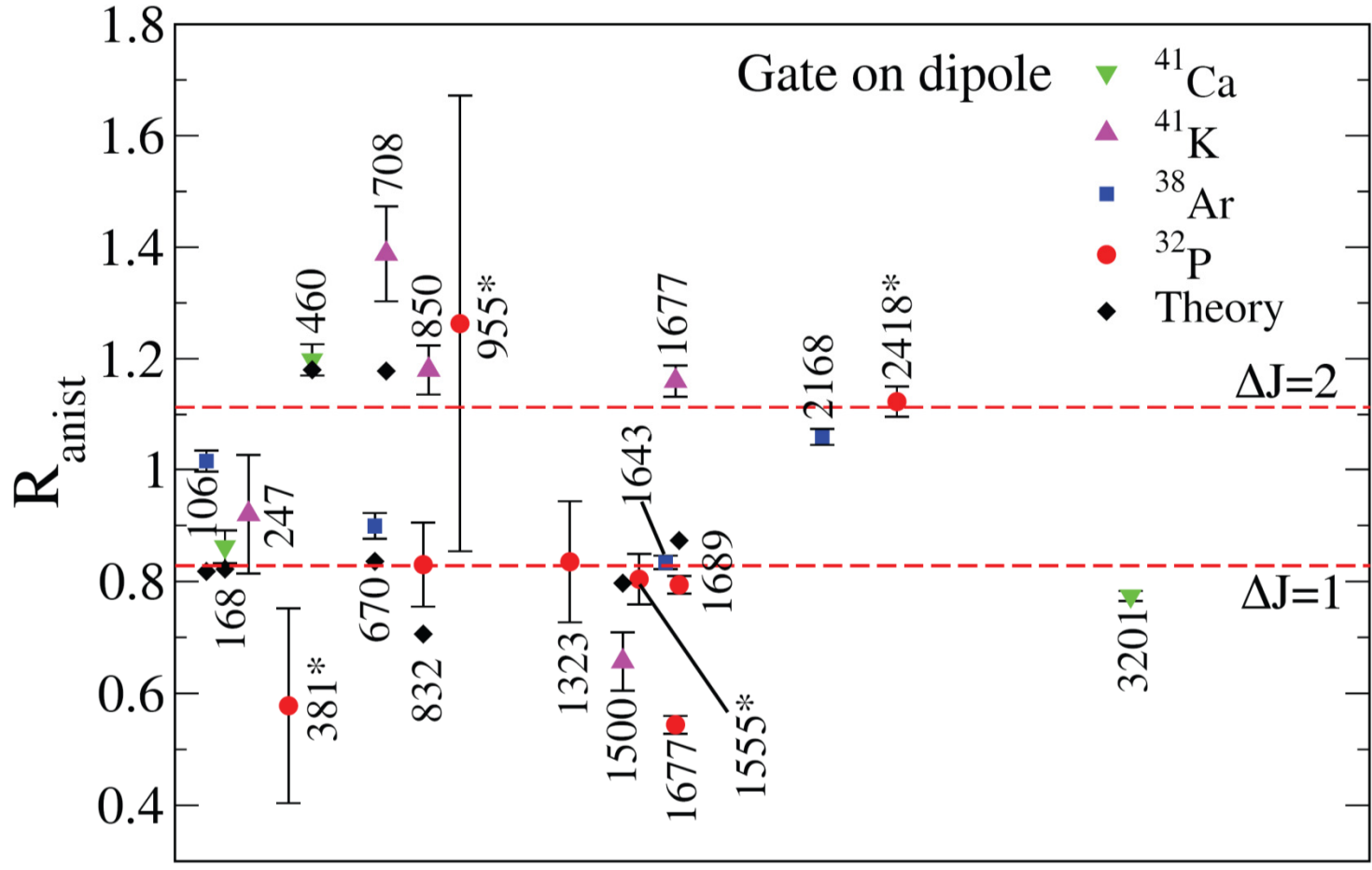
Alternative Method

Determination of Multipolarity

$^{16}\text{O} + ^{18}\text{O} @ 34\text{MeV}$

Asymmetric γ - γ matrices:
 57° Vs 90°
 32° Vs 90°

$$R_{\text{anist}} = \frac{I_{\gamma_1 \text{ at } 32^\circ, \text{ gated with } \gamma_2 \text{ at } 90^\circ}}{I_{\gamma_1 \text{ at } 57^\circ, \text{ gated with } \gamma_2 \text{ at } 90^\circ}}$$

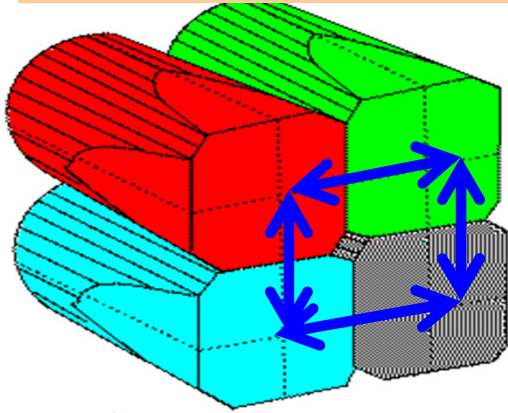


Calibration points:
 Transitions with known multiplicities in other strongly populated nuclei exhibiting no lineshape

Theoretical calculations done using code: ANGCOR

Magnetic or Electric??

- ✓ Electric transition results in a preferential scattering in perpendicular direction (with respect to the reaction plane).
- ✓ While a magnetic transition indicates a preferential scattering in parallel direction.

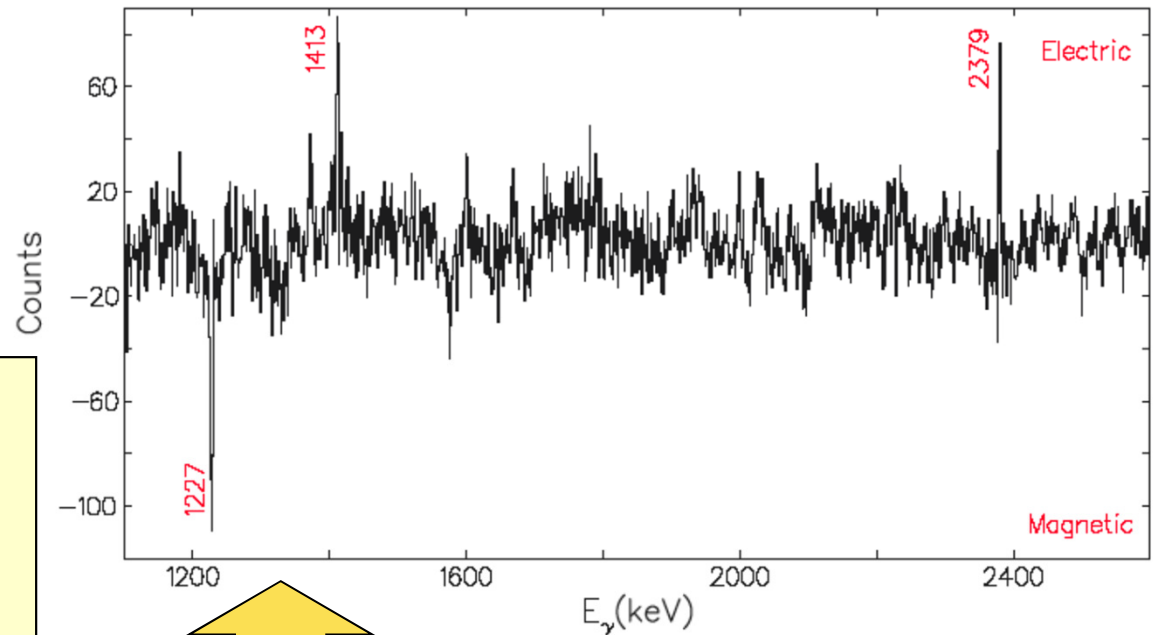


Clover detector has *uniquely* facilitated polarization measurements. Each crystal acts as a scatterer while the adjacent crystals act as absorbers.

Background subtracted difference spectrum for perpendicular and parallel coincidences in ^{33}P (gate on 1848 keV). The electric γ -ray transition shows positive peak, whereas the magnetic γ -ray transition shows negative peak.

Asymmetric matrices generated:

- One axis corresponds to perpendicular or parallel scattered events in clovers at 90°
- Other axis corresponds to total energy deposited in any of the other detectors.



Experimental Linear Polarization measurement

$$\Delta_{IPDCO} = \frac{aN_{\perp} - N_{\parallel}}{aN_{\perp} + N_{\parallel}}$$

N_{\perp} = Number of photons with a given energy scattered along the direction \perp to the reaction plane

N_{\parallel} = Number of photons with a given energy scattered along the direction \parallel to the reaction plane

$$a = \frac{N_{\parallel}(\text{unpolarized})}{N_{\perp}(\text{unpolarized})}$$

$$P_{\text{exp}}(\theta) = \Delta/Q,$$

Theoretical Polarization measurement

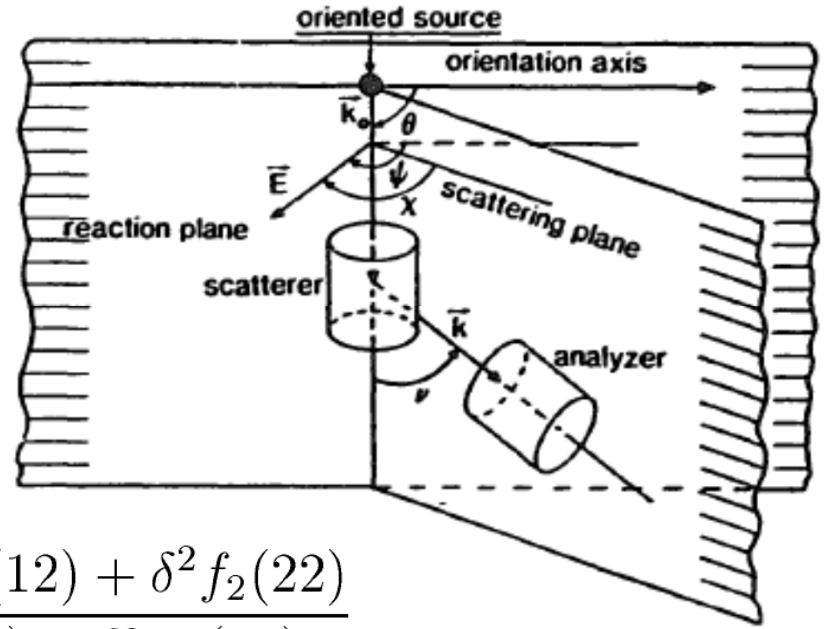
$$P_{\text{cal}}(90^{\circ}) = \pm \frac{3a_2H_2 - 7.5a_4H_4}{2 - a_2 + 0.75a_4}$$

H_2 and H_4 are linear polarization mixing coefficients
(Derived for $L = 2$, $L' = 3$ transitions)

a_2 and a_4 are angular distribution coefficients

$$P(\theta) = \frac{W(\theta, \psi = 0) - W(\theta, \psi = \pi/2)}{W(\theta, \psi = 0) + W(\theta, \psi = \pi/2)}$$

$$P_{cal}(90^\circ) = \pm \frac{3a_2H_2 - 7.5a_4H_4}{2 - a_2 + 0.75a_4}$$

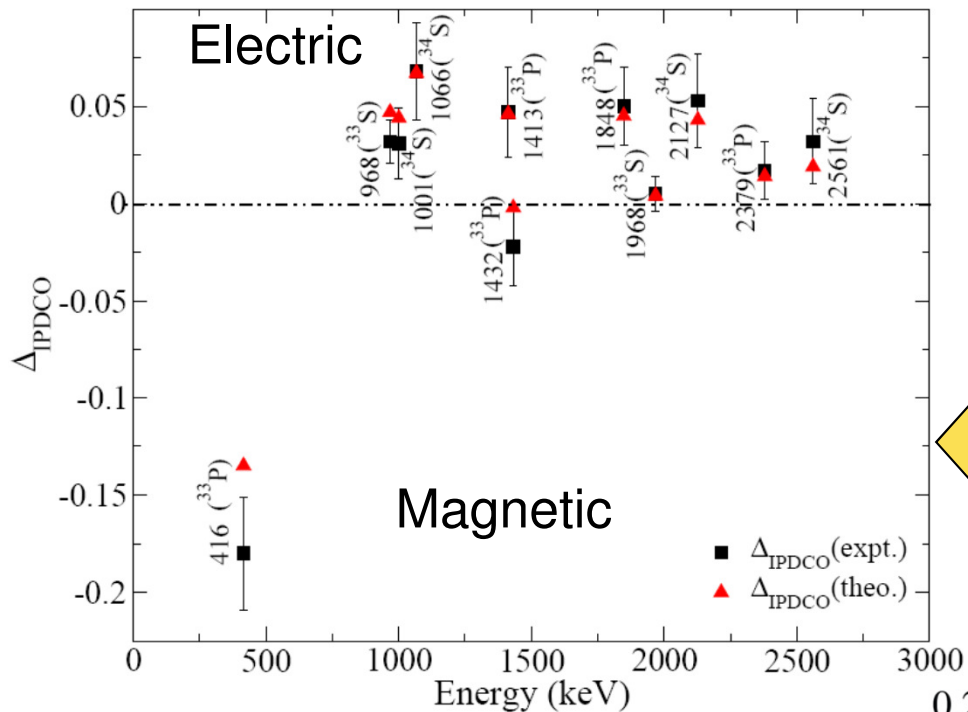


$$H_2(L = 1, L' = 2) = \frac{f_2(11) - (2/3)\delta f_2(12) + \delta^2 f_2(22)}{f_2(11) + 2\delta f_2(12) + \delta^2 F_2(22)}$$

$$H_4(L = 1, L' = 2) = -1/6$$

$$H_2(L = 2, L' = 3) = \frac{-f_2(22) - \delta f_2(23) + (2/3)\delta^2 f_2(33)}{f_2(22) + 2\delta f_2(23) + \delta^2 f_2(33)}$$

$$H_4(L = 2, L' = 3) = \frac{5f_4(22) - 2\delta f_4(23) + 20\delta f_4(33)}{30(f_4(22) + 2\delta f_4(23) + \delta^2 f_4(33))}$$



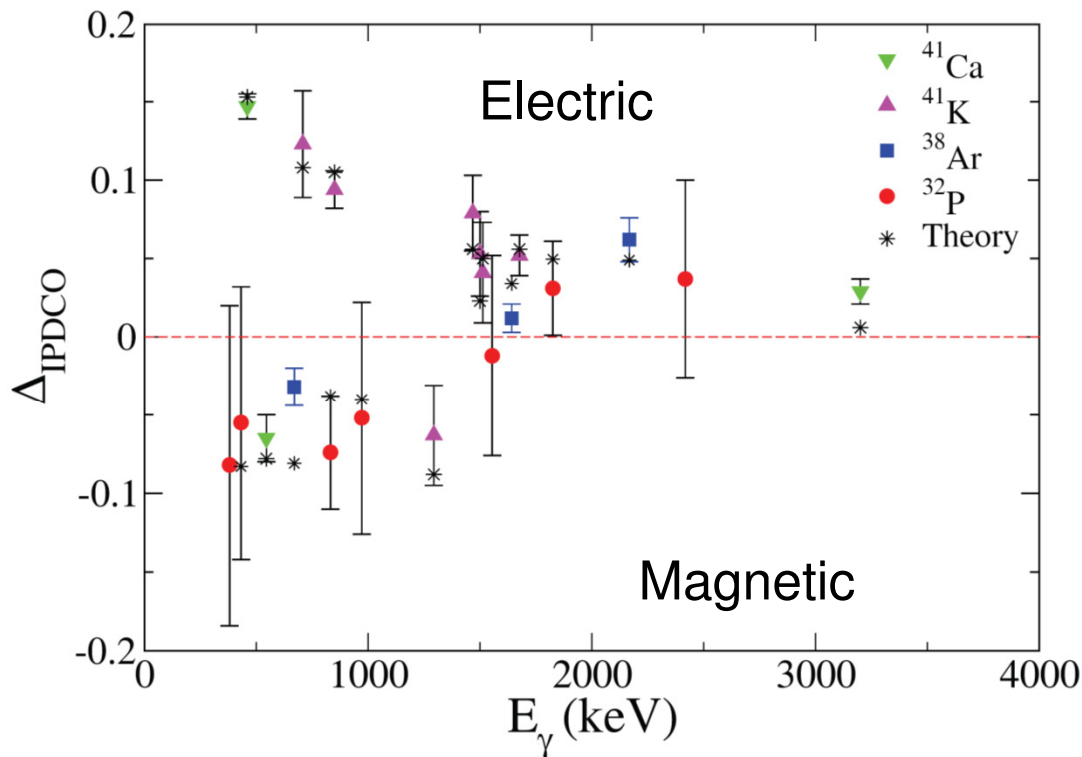
$\Delta_{IPDCO} = +ve \longrightarrow$ **Electric**
 $= -ve \longrightarrow$ **Magnetic**
 $\sim 0 \longrightarrow$ **Mixed**

$^{18}\text{O} + ^{18}\text{O}$ @ 34 MeV

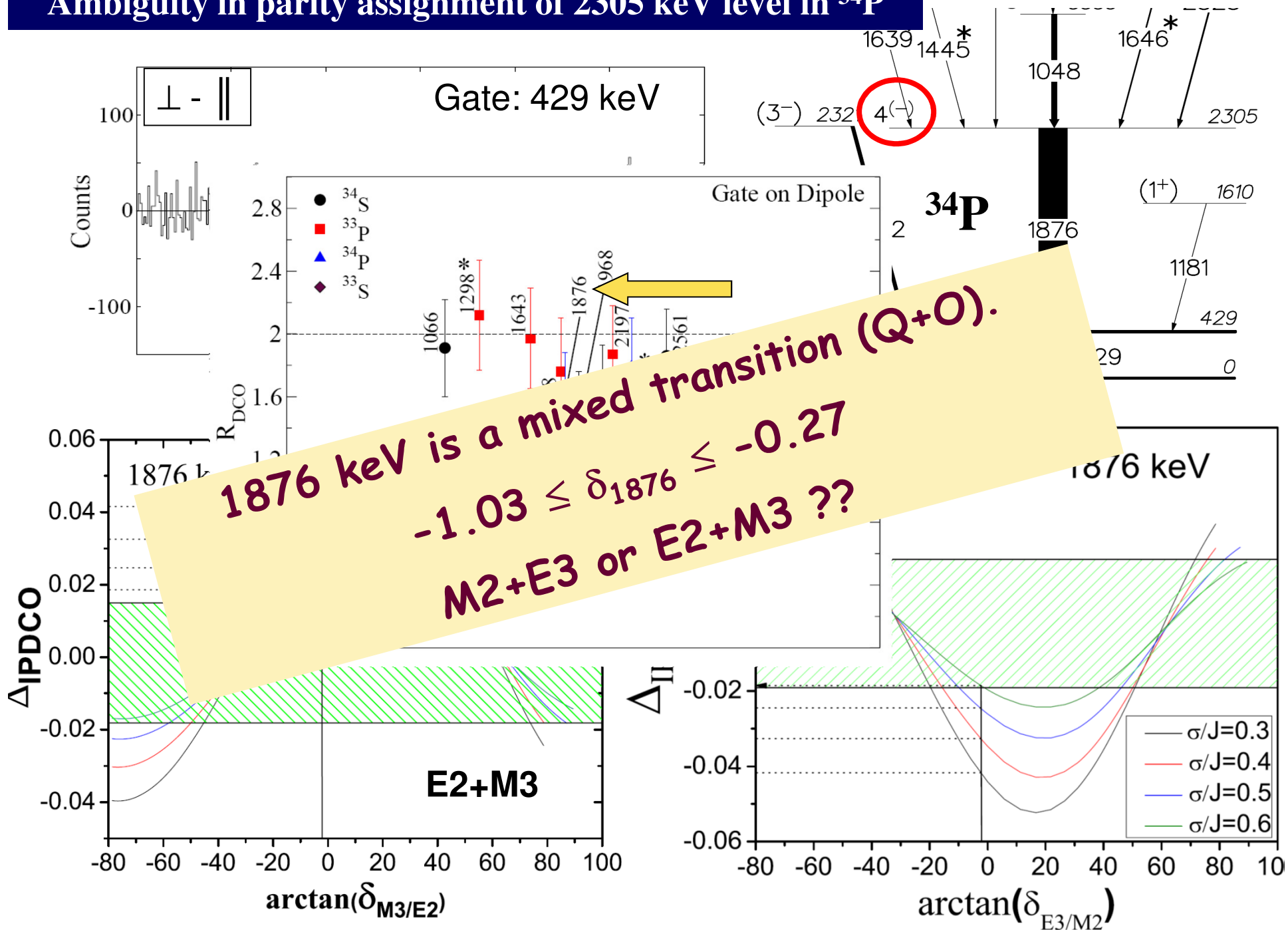
$$\pi(ML) = (-1)^{L+1}$$

$$\pi(EL) = (-1)^L$$

$^{16}\text{O} + ^{18}\text{O}$ @ 34 MeV



Ambiguity in parity assignment of 2305 keV level in ^{34}P



Lifetime of 2305 keV level : $0.3\text{ns} \leq t_{1/2} \leq 2.5\text{ns}$ [1]

Half-life (ns)	Mixing ratio (δ)	Reduced transition probabilities			
		$M2/E3$		$E2/M3$	
		$B(M2)$ (W.u.)	$B(E3)$ (W.u.)	$B(E2)$ (W.u.)	$B(M3)$ (W.u.)
0.3	-1.03	0.207	372.681	0.006	12520.654
	-0.27	0.397	49.191	0.012	1652.638
2.5	-1.03	0.025	44.722	0.001	1502.478
	-0.27	0.048	5.903	0.001	198.317

Conclusion:
1876 keV is plausibly a M2+E3 transition
2305 keV level : $J^\pi = 4^-$

- [1] M. Asai, T. Ishii, A. Makishima, M. Ogawa, and M. Matsuda, in *Proceedings of the Third International Conference on Fission and Properties of Neutron-Rich Nuclei*, edited by J. H. Hamilton, A. V. Ramayya, and H. K. Carter (World Scientific, Singapore, 2002), pp. 295–297.

Half-life of the $I^\pi = 4^-$ Intruder State in ^{34}P : $M2$ Transition Strengths Approaching the Island of Inversion.

P.J.R Mason^{a,*}, T. Alharbi^{a,b}, P.H. Regan^a, N. Mărginean^c, Zs. Podolyák^a,
N. Alkhomashi^d, P.C. Bender^e, M. Bowry^a, M. Bostan^f, D. Bucurescu^c,
A.M. Bruce^g, G. Căta-Danil^c, I. Căta-Danil^c, R. Chakrabarti^h, D. Deleanu^c,
P. Detistovⁱ, M.N. Erduran^j, D. Filipescu^c, U. Garg^k, T. Glodariu^c,
D. Ghiță^c, S.S. Ghugre^h, A. Kusoglu^f, R. Mărginean^c, C. Mihai^c,
M. Nakhostin^a, A. Negret^c, S. Pascu^c, C. Rodríguez Triguero^g, T. Sava^c,
E.C. Simpson^a, A.K. Sinha^h, L. Stroe^c, G. Suliman^c, N.V. Zamfir^c

^a*Department of Physics, University of Surrey, Guildford, Surrey GU2 7XH, UK*

^b*Department of Physics, Almajmaah University, P.O. Box 66, 11952, Saudi Arabia*

^c*Horia Hulubei National Institute of Physics and Nuclear Engineering (IFIN-HH),
R-76900 Bucharest, Romania*

^d*KACST, P.O Box 6086, Riyadh 11442, Saudi Arabia*

^e*Department of Physics, Florida State University, Tallahassee, Florida, USA*

^f*Department of Physics, Istanbul University, 34134 Istanbul, Turkey*

^g*School of Computing, Engineering and Mathematics, University of Brighton, Brighton,
BN2 4GJ, UK*

^h*UGC-DAE Consortium for Scientific Research, Kolkata Centre, Kolkata 700098, India*

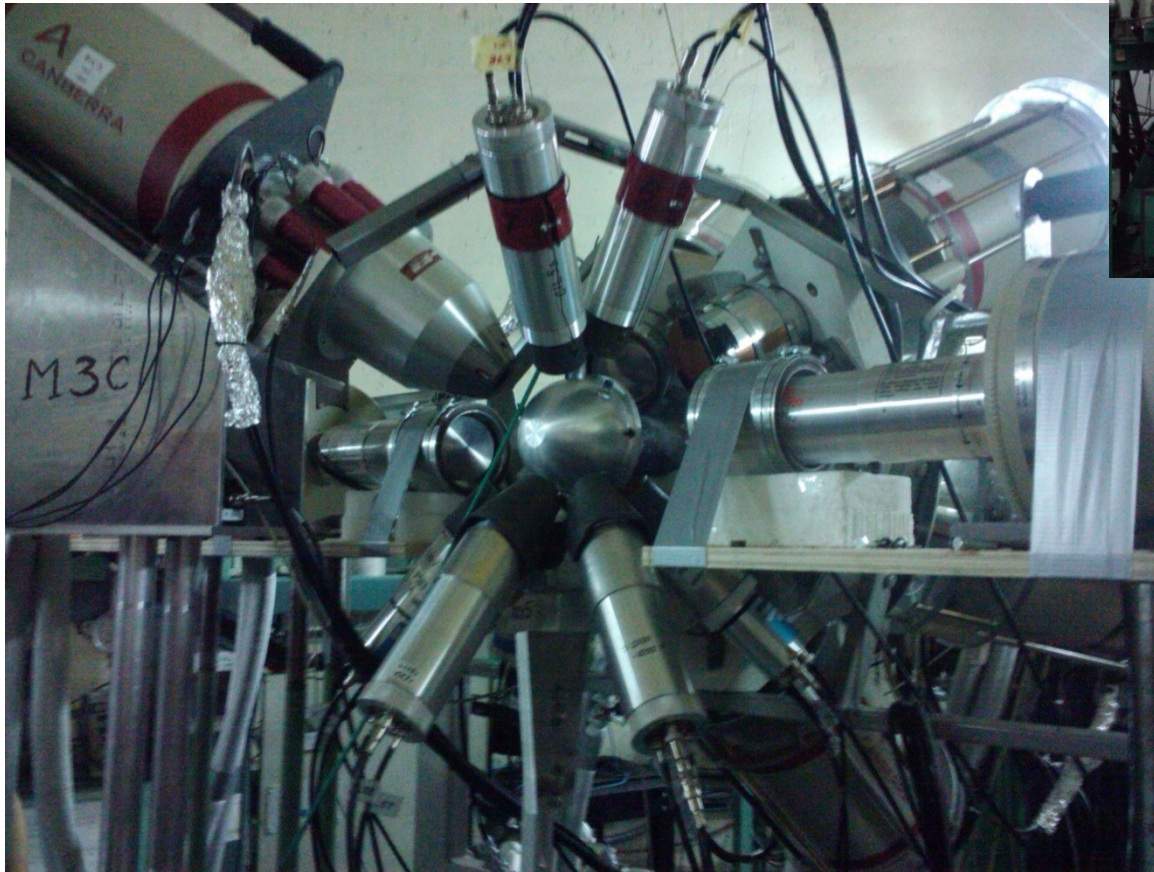
ⁱ*Institute for Nuclear Research and Nuclear Energy (INRNE), Bulgarian Academy of
Sciences, Sofia, Bulgaria*

^j*Department of Computer Engineering, Istanbul Sabahattin Zaim University, Istanbul,
Turkey*

^k*Department of Physics, University of Notre Dame, Notre Dame, Indiana, 46556, USA*

Experiment

50mg/cm² Ta₂¹⁸O Enriched foil
¹⁸O Beam from Bucharest Tandem
(~20pA)



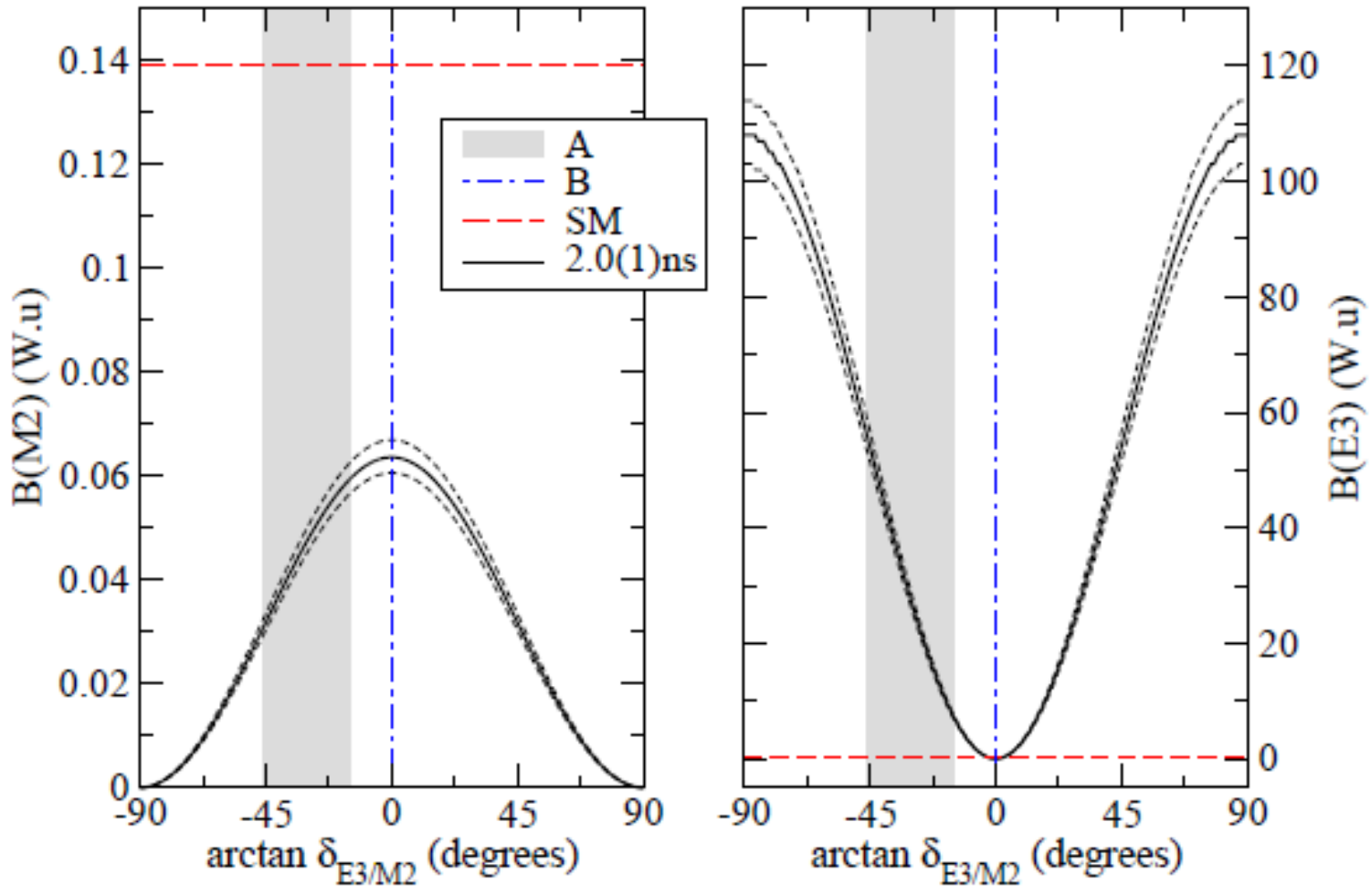
Array 8 HPGe
(unsuppressed) and 7
LaBr₃:Ce detectors

-3 (2"x2") cylindrical
-2 (1"x1.5") conical
-2 (1.5"x1.5") cylindrical

Abstract

The half-life of the $I^\pi = 4^-$ intruder state in ^{34}P has been measured as $t_{1/2} = 2.0(1)$ ns using γ -ray coincidence, fast-timing techniques with the Bucharest HPGe and $\text{LaBr}_3:\text{Ce}$ detector array. Excited states in ^{34}P were populated using the $^{18}\text{O}(^{18}\text{O},\text{pn})^{34}\text{P}$ fusion-evaporation reaction at a beam

- **Theoretical predictions suggest**
 - **2^+ state based primarily on $[\pi 2s_{1/2} \times (\nu 1d_{3/2})^{-1}]$ configuration and**
 - **4^- state based primarily on $[\pi 2s_{1/2} \times \nu 1f_{7/2}]$ configuration.**
- **Thus expect transition to go mainly via $f_{7/2}$ -to- $d_{3/2}$, M2 transition.**
- **Different admixtures in 2^+ and 4^- states allow mixed M2/E3 transition**

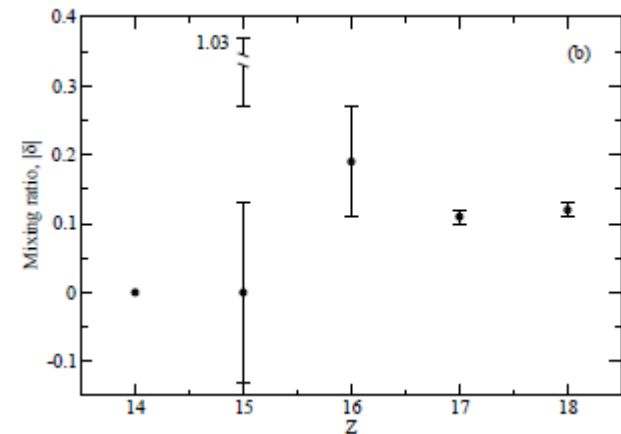
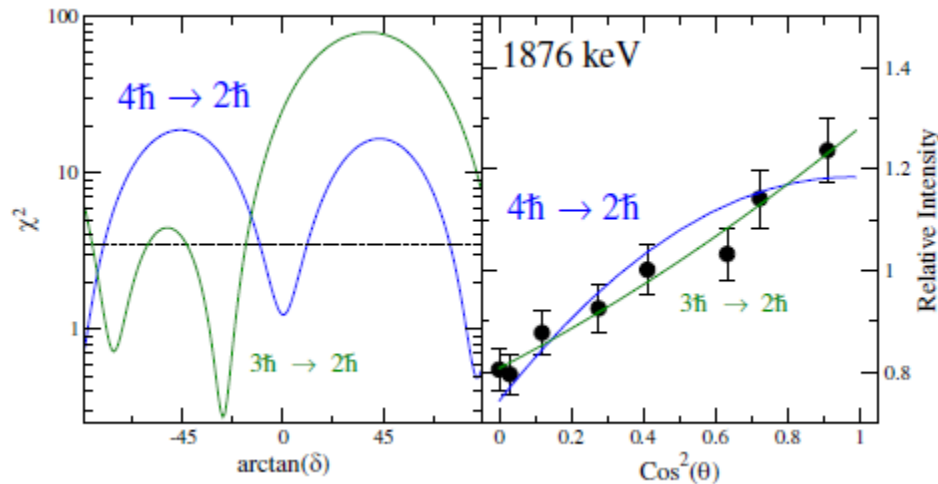


[8] P.C. Bender *et al.*, in preparation (unpublished).

Table 6.13: Summary of experimental data on ^{34}P . The B values are for the indicated multipolarity λ . In some cases more than one possible spin in compared to theory.

E_x (keV)	E_γ (keV)	J_n^π initial	J_n^π final	Branch (%)	Mean τ (ps)	a_2	a_4	$\arctan(\delta)$ (deg.)	λ	B value (W.u.)	WBP-a (W.u.)	SDPF-s (W.u.)
429	429	2_1^+	1_1^+	100	1.9(+9/-5)	-0.087	0.021	-5	M1	0.21(+8/-7)	0.33	
1608	1179	1_2^+	2_1^+	66	0.75(+65/-20)	-0.033	0.005		M1	0.017(+6/-7)	0.005	
	1607		1_1^+	34					M1	.004(+1/-2)	0.001	
2229	621	2_1^-	1_2^+	30	> 2.8	-0.121	0.064	-3	E1	$< 4 \cdot 10^{-4}$		
	1800		2_1^+	44					E1	$< 2.5 \cdot 10^{-5}$		
	2229		1_1^+	26					E1	$< 8 \cdot 10^{-6}$		
2305	1876	4_1^-	2_1^+	100	2900(290)	0.319	0.015	0	M2	0.064(6)	0.15	
2320	1891	3_1^-	2_1^+	100	> 10	-0.146	0.032	-3	E1	$< 1.5 \cdot 10^{-4}$		

6



Theory

Results



wbp-a



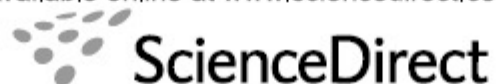
sdpf-m

sdpf-mw





Available online at www.sciencedirect.com



Nuclear Physics A 847 (2010) 149–167

www.elsevier.com/locate/nuclphysa

Cross-shell excitations in ^{30}Al and ^{30}Si at high spin

D. Steppenbeck^{a,*}, A.N. Deacon^a, S.J. Freeman^a, R.V.F. Janssens^b,
M.P. Carpenter^b, C.R. Hoffman^{c,1}, B.P. Kay^{a,1}, T. Lauritsen^b,
C.J. Lister^b, D. O'Donnell^{d,2}, J. Ollier^{d,2}, D. Seweryniak^b, J.F. Smith^d,
K.-M. Spohr^d, S.L. Tabor^c, V. Tripathi^c, P.T. Wady^d, S. Zhu^b

^a *Schuster Laboratory, University of Manchester, Manchester M13 9PL, UK*

^b *Argonne National Laboratory, Argonne, IL 60439, USA*

^c *Department of Physics, Florida State University, Tallahassee, FL 32306, USA*

^d *Department of Physics, University of the West of Scotland, Paisley PA1 2BE, UK*

Received 24 May 2010; received in revised form 2 July 2010; accepted 26 July 2010

Available online 14 August 2010

^{30}Al

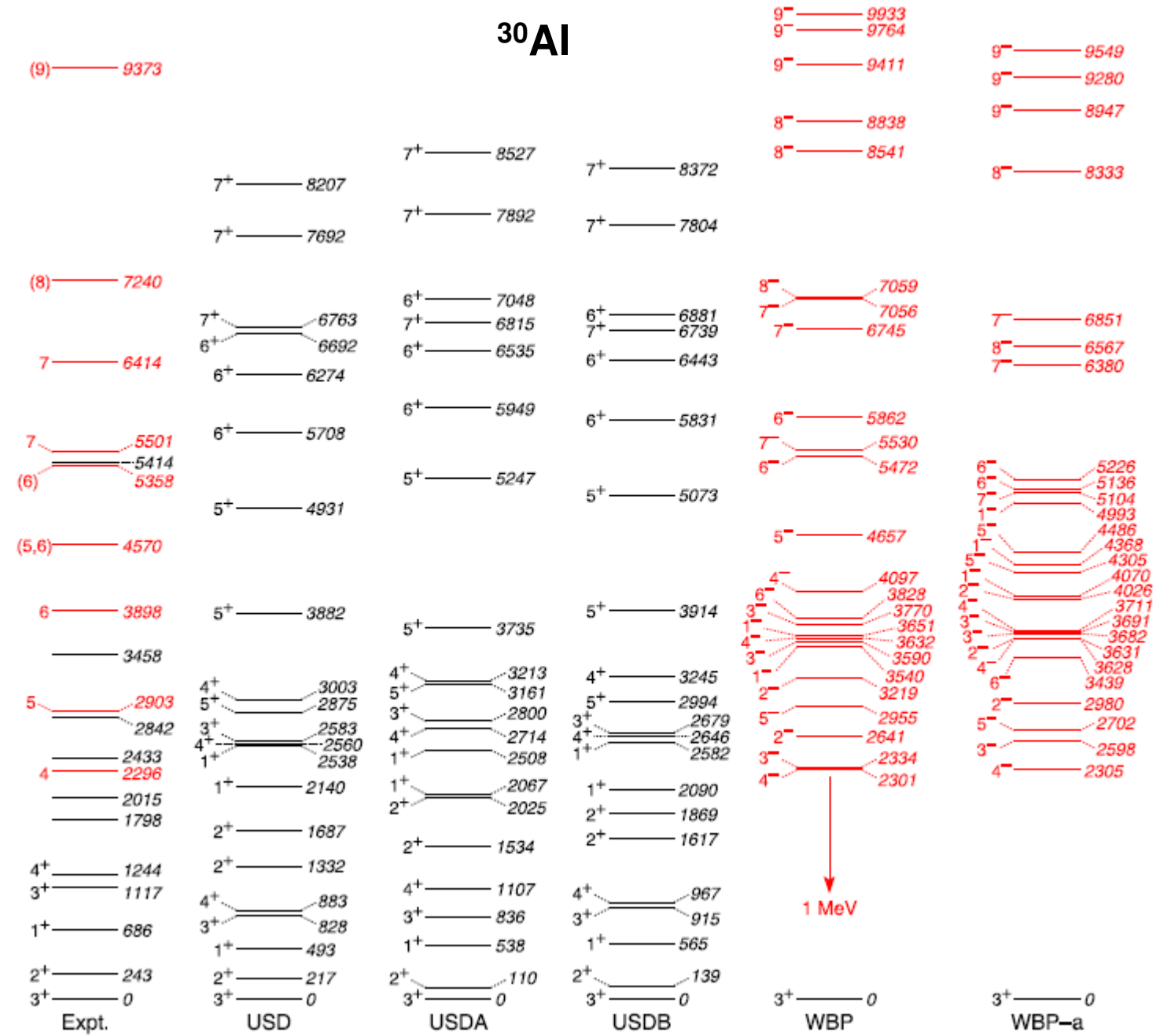


Figure 1: Energy level diagrams for ^{30}Al showing experimental data and theoretical calculations from USD, USDA, USDB, WBP, and WBP-a models.

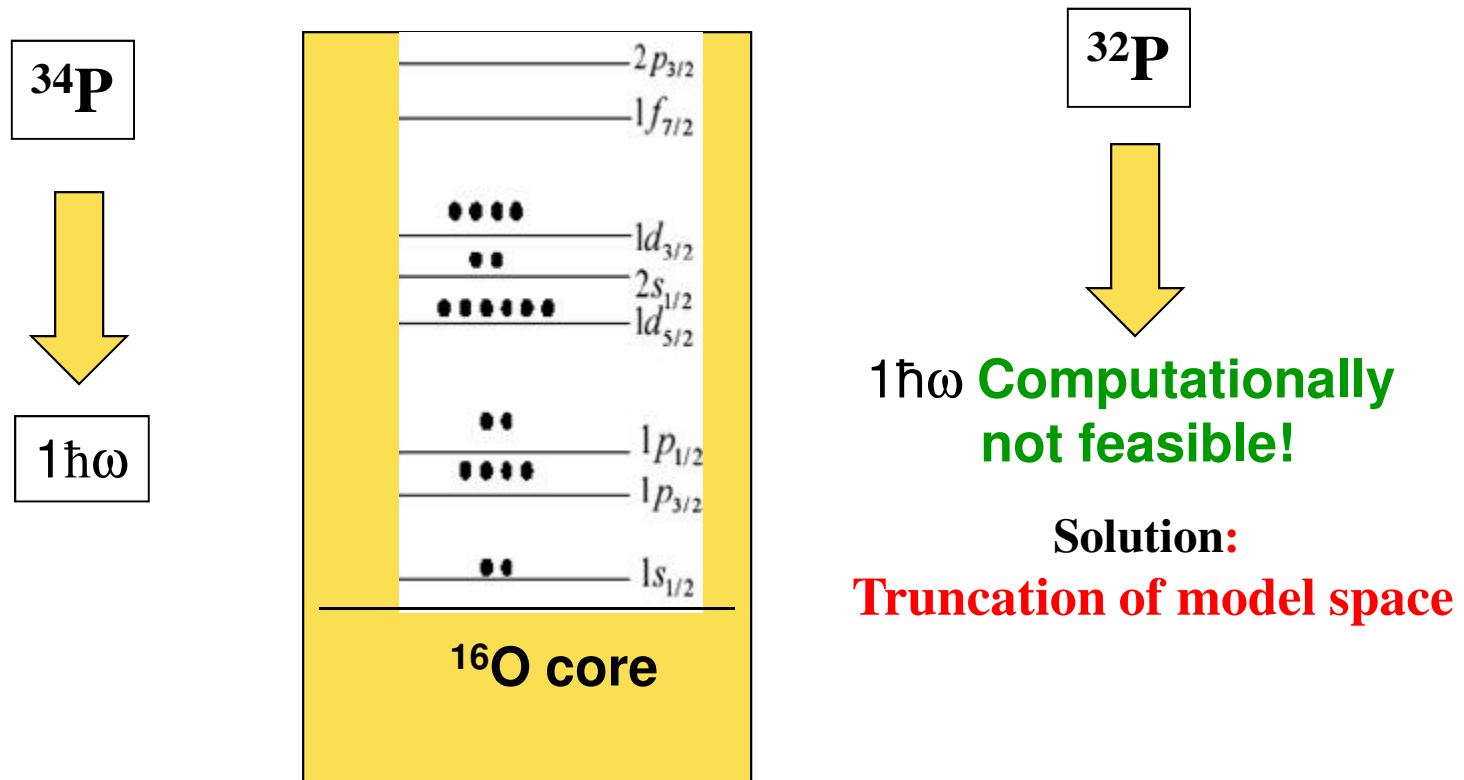
Such observations imply that the energies of the negative parity states are, to a good approximation, simple reduced by a common quantity with increasing neutron number, this may be naively interpreted as a reduction in the magnitude of the energy gap between the neutron Fermi surface and the fp shell.

Shell Model calculations using Nushell Code

Interaction: *sdpfmw*

For positive parity states:
Calculations with full *sd* shell as valence space outside ^{16}O core

For negative parity and high-lying positive parity states:
Desired valence space: Full *sdpf* outside ^{16}O core.

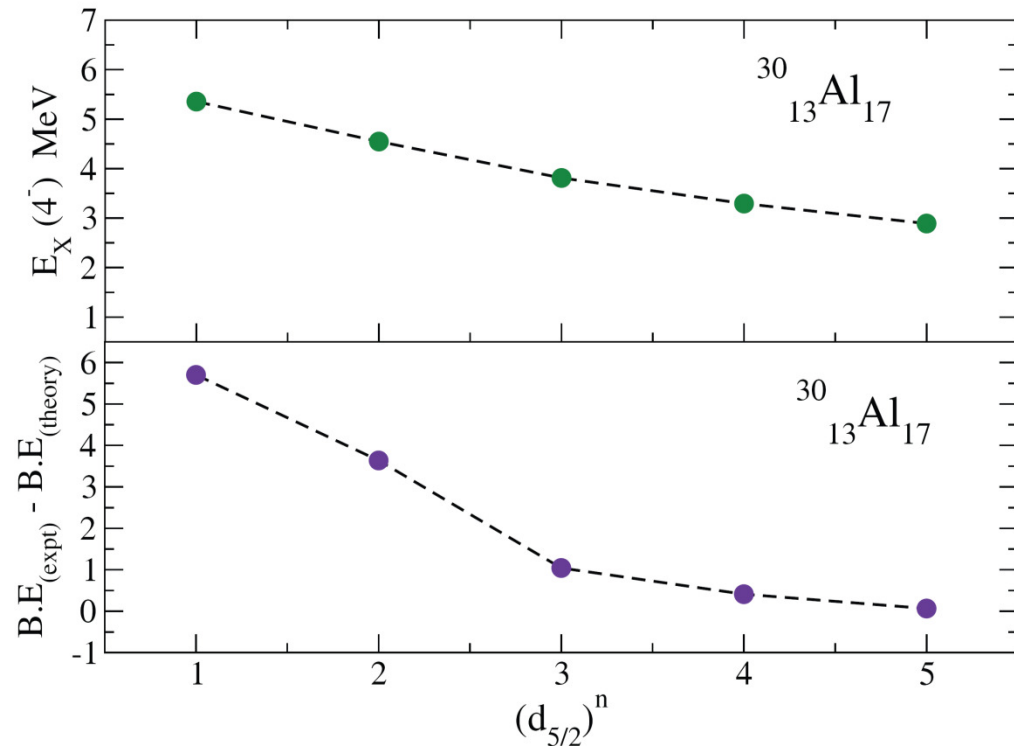


Possible reasons behind the need to lower SPEs

- Inappropriate choice of Two-Body-Matrix-Elements.
 - The TBME used may not be optimized for this region.
- Truncation of the model space
 - The truncation of the model space renders the ground state less bound, resulting in the excitation energies occurring at higher values compared to their experimental counterpart

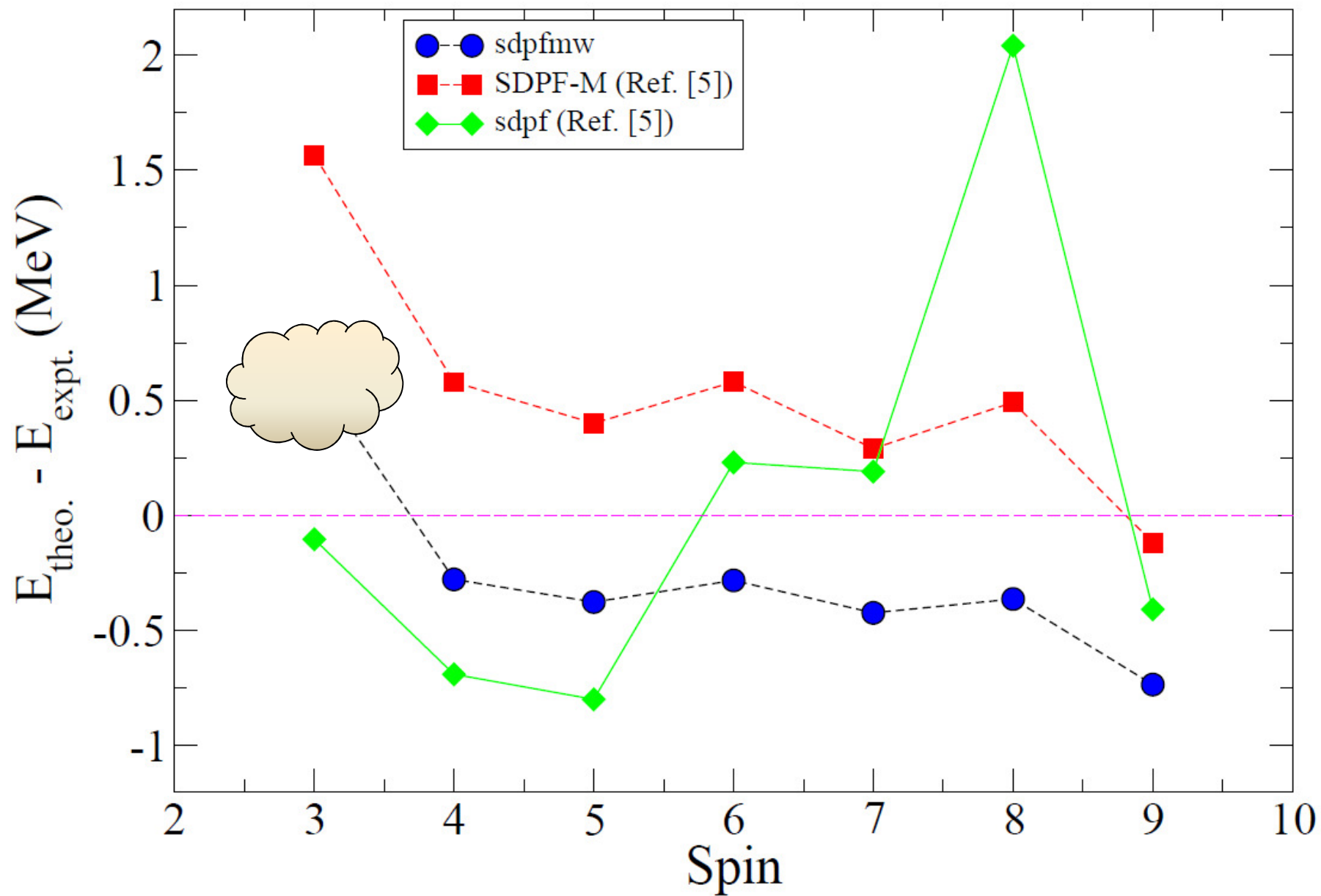
Warburton *et al.* (Phys. Rev. C 41, 1147 (1990)) have developed an interaction which

- Optimized for $A = 29 - 44$
- Includes the necessary ingredients for the cross-shell terms

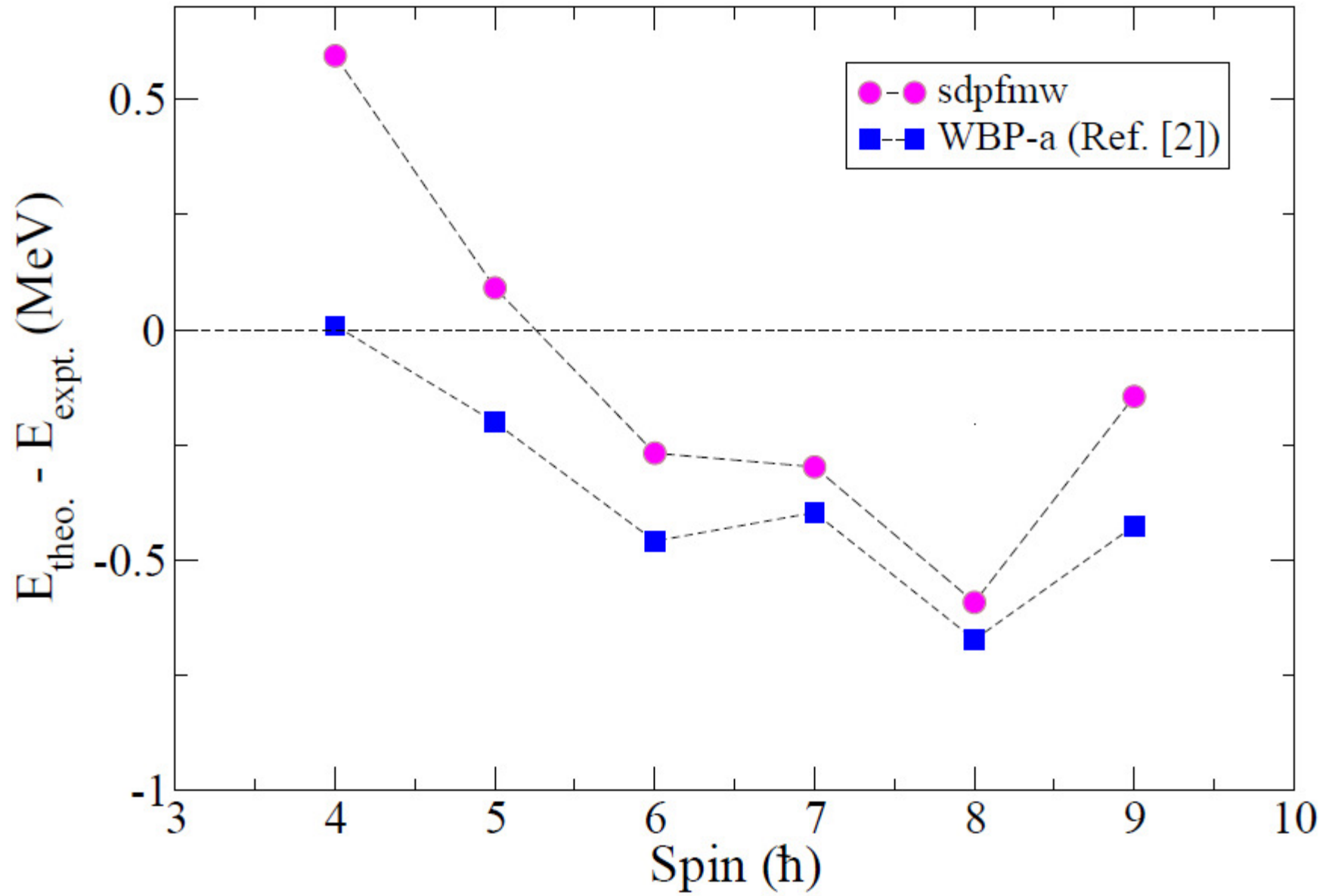


^{34}S

Phys. Rev. C 71, 014316 (2005)

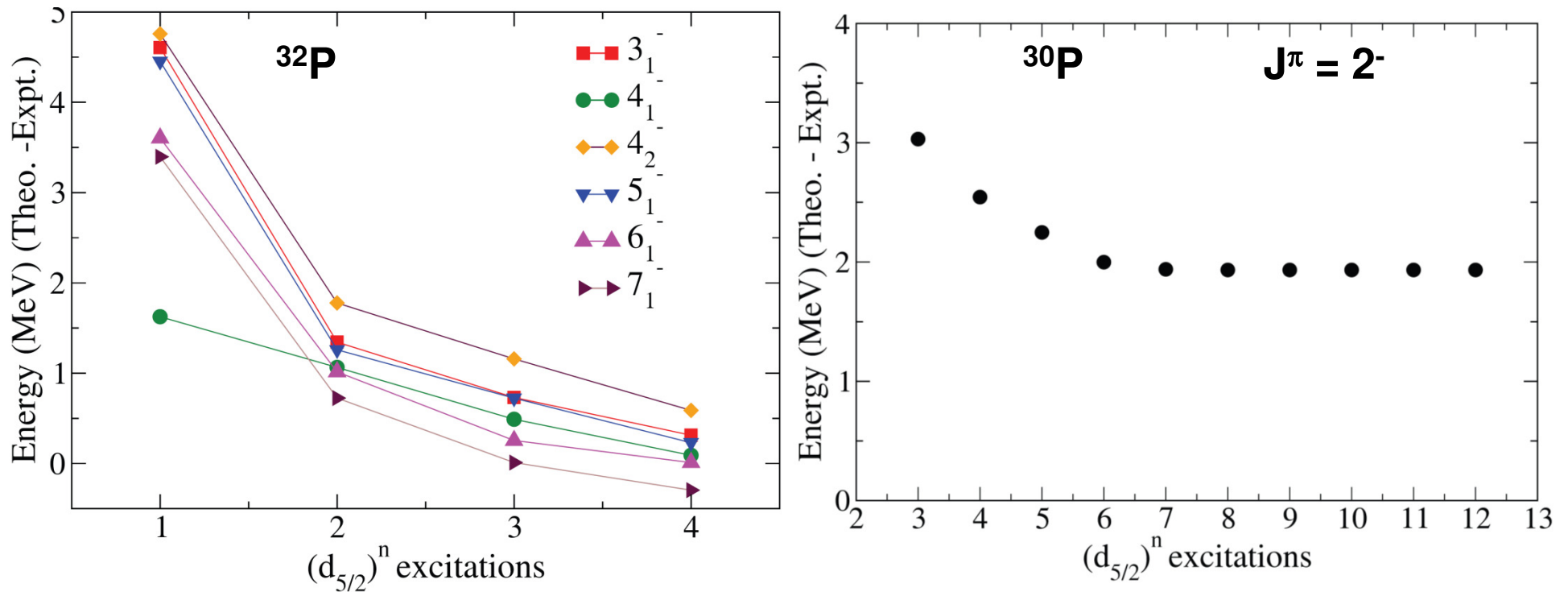


^{30}Al



Sdpmw interaction

No need for lowering SPE of $f_{7/2}$ or $p_{3/2}$



Plot of the difference between experimental and shell model predicted excitation energy of the negative parity states as a function of the number of particles (n) excited from $1d_{5/2}$ orbital in $^{30}, ^{32}\text{P}$.

0hω	
6 ⁺ <u>7670</u>	7 ⁻ <u>7099</u>
7 ⁺ <u>6237</u>	5 ⁺ <u>6509</u>
	3 ⁺ <u>6449</u>
	4 ⁺ <u>6308</u>
	3 ⁺ <u>6156</u>
	3 ⁺ <u>5806</u>
	0 ⁻ <u>5465</u>
	6 ⁻ <u>5207</u>
	1 ⁺ <u>5024</u>
6 ⁽⁻⁾ <u>4630</u>	3 ⁺ <u>4719</u>
	2 ⁺ <u>4406</u>
	5 ⁻ <u>4532</u>
	1 ⁻ <u>4251</u>
5 ⁽⁻⁾ <u>3951</u>	1 ⁺ <u>4233</u>
	4 ⁺ <u>3788</u>
	5 ⁻ <u>4122</u>
5 ⁽⁻⁾ <u>3353</u>	2 ⁻ <u>3351</u>
	2 ⁺ <u>3176</u>
	1 ⁺ <u>2953</u>
	4 ⁻ <u>2756</u>
(3 ⁻) <u>2321</u>	3 ⁺ <u>2737</u>
4 ⁽⁻⁾ <u>2305</u>	3 ⁻ <u>2737</u>
	2 ⁺ <u>2216</u>
1 ⁺ <u>1609</u>	0 ⁺ <u>1487</u>
	1 ⁺ <u>1408</u>
	1 ⁺ <u>0</u>
2 ⁺ <u>429</u>	2 ⁺ <u>362</u>
1 ⁺ <u>0</u>	1 ⁺ <u>0</u>
Experimental	Shell Model (sdpf calculations)

1h ω

Nushell calculations “sdpfmw interaction”

Valence space consists of
 $1d_{5/2}$, $2s_{1/2}$, $1d_{3/2}$, $1f_{7/2}$, $2p_{3/2}$, $1f_{5/2}$, $2p_{1/2}$
 outside ^{16}O core

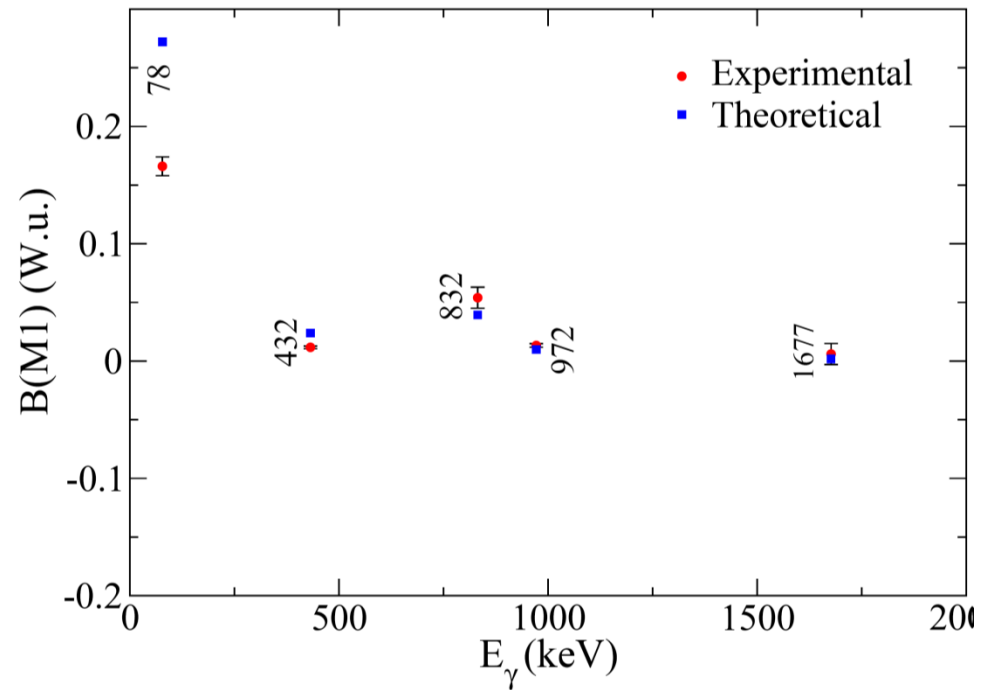
^{34}P : Comparison between theory & experiment in present work

			(8 ⁻) 9637	8 ⁻ 9285
	7 ⁺ 8823	7 ⁺ 8901		
	6 ⁺ 7392	6 ⁺ 7452	7 7417	7 ⁻ 7122
			(6 ⁻) 6814	6 ⁻ 6953
	5 ⁺ 5614	5 ⁺ 5731	6 ⁽⁻⁾ 5862	5 ⁻ 6008
			5 ⁽⁻⁾ 5481	6 ⁻ 5873
	5 ⁺ 4976	5 ⁺ 5079		4 ⁻ 5286
4698				5 ⁻ 4507
4 ⁺ 4036			5 ⁻ 4276	
	4 ⁺ 3727	4 ⁺ 3894		3 ⁻ 3634
4 ⁺ 3149	4 ⁺ 3167	4 ⁺ 3212	4 ⁻ 3444	4 ⁻ 3535
	3 ⁺ 2916	3 ⁺ 3011	3 ⁻ 3321	
3 ⁺ 2177	3 ⁺ 2224	3 ⁺ 2287		
3 ⁺ 1755				
	3 ⁺ 1527	3 ⁺ 1571		
2 ⁺ 1323	2 ⁺ 1135	2 ⁺ 1147		
2 ⁺ 78	1 ⁺ 5	2 ⁺ 5		
1 ⁺ 0	2 ⁺ 0	1 ⁺ 0		
Expt.	Theo. I	Theo. II	Expt.	Theo. II

³²P: Comparison between theory & experiment in present work

Truncation:

$$d_{5/2}^{(8-12)} s_{1/2}^{(0-4)} d_{3/2}^{(0-8)} f_{7/2}^{(0-1)}$$



Experimental E3/M2 mixing ratios could not be predicted by Shell model for N =19 nuclei

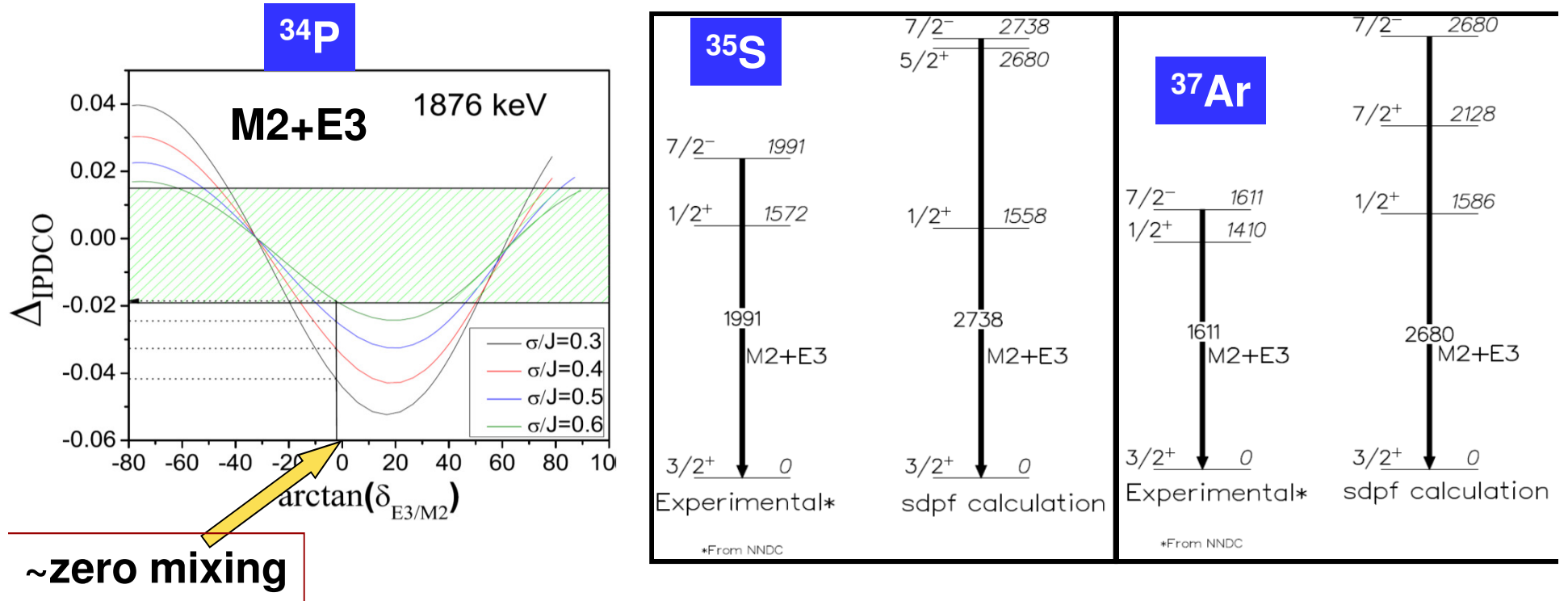


TABLE IV: Comparison between experimental and theoretical transition energies, excitation energies, mixing ratios and reduced transition probabilities in ^{35}S and ^{37}Ar .

E_γ [keV]		$E_x(J^\pi)$ [keV]		τ [ns]	δ		$B(M2)$ [W.u.]		$B(E3)$ [W.u.]	
Expt.	Theo.	Expt.	Theo.	from NNDC	Expt.	Theo.	Expt.	Theo.	Expt.	Theo.
^{35}S										
1991	2738	1991	2738	1.02(5)	-0.19(8)	-0.05	0.088(5)	0.196	4.62	0.38
^{37}Ar										
1611	2680	1611	2680	4.37(9)	-0.12(1)	-0.08	0.058(13)	0.112	1.7(3)	0.50

CONCLUSION

- ❑ Use of **heavy-ion fusion reaction** has resulted in population of high spin states.
- ❑ The **1876-keV transition** de-exciting the 2305-keV level in ^{34}P was confirmed to be a **mixed transition** with a plausible **M2/E3 admixture**.
- ❑ **Shell model calculations**
 - ❑ **successfully reproduced** low-lying positive and negative parity states.
 - ❑ **No lowering of single particle energy** as carried out by other workers.
 - ❑ Omission of **important configurations** responsible for **prediction of E_x at higher energies** compared to their experimental counterpart; as these **get included** theory approaches experiment.
- ❑ Shell model calculations reasonably successful in predicting the wave functions except in few cases, particularly the M2/E3 mixing in N=19 isotones.
- ❑ Need to perform the calculations within a larger model space and/or with an appropriate Hamiltonian (which includes microscopic intra- and inter shell interactions.)

Shell model is successful in explaining the overall Structure with certain interesting exceptions



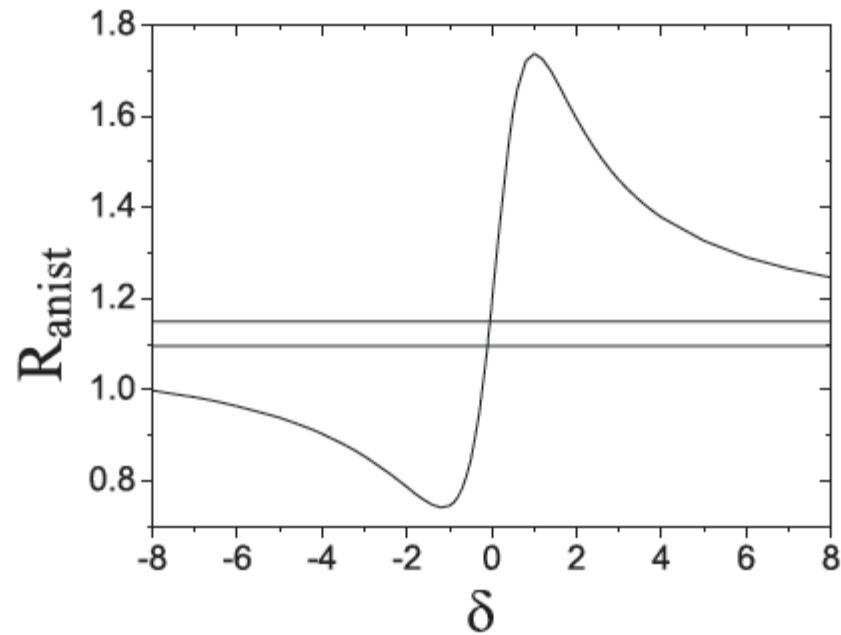


FIG. 7. Plot of the calculated R_{anist} as a function of mixing ratio for a $J = 6 \rightarrow 4$ transition. The area between the horizontal lines represent the uncertainty in the observed R_{anist} of the 2418-keV transition.